The thesis committee for Hussein A. Hachem
Certifies that this is the approved version of the following thesis:

Modeling of pore pressure propagation and dissipation in compressible porous media

APPROVED BY
SUPERVISING COMMITTEE:

Chadi El Mohtar, co-supervisor

Robert Gilbert, co-supervisor

Modeling of Pore Pressure Propagation and Dissipation in Compressible Porous Media

by

Hussein A. Hachem, B.E.

Thesis

Presented to the Faculty of the Graduate School of

The University of Texas at Austin

in Partial Fulfillment

of the Requirements

for the Degree of

Master of Science in Engineering

The University of Texas at Austin

May 2017

Dedication

To the most awesome parents in the world

Sanaa Barakat and Abdel Latif Hachem

Acknowledgements

I would like to express my gratitude to Drs. Chadi El Mohtar and Robert Gilbert for their continuous support of this work and the effort that was made to complete it. Their guidance made this thesis possible. I would also like to thank Dr. Jorge Zornberg for his contribution as a reader.

I extend my thanks to everyone at the University of Texas at Austin, specifically in the civil engineering department, whom I met during graduate school. I have learnt a lot from every single one of the faculty, fellow students and staff. My deep gratitude also goes to the American University of Beirut, my undergraduate alma mater, who forged my love for geotechnical engineering.

Abstract

Modeling of Pore Pressure Propagation and Dissipation in Compressible Porous Media

Hussein A. Hachem, M.S.E

The University of Texas at Austin, 2017

Supervisors: Chadi El Mohtar and Robert Gilbert

This research is a study of the different phenomena associated with the propagation of pore water pressure in high plasticity clays. Specifically, it addresses the pore pressure response in areas subjected to sudden increases in pore water pressure at their top boundary. The main applications of this research would be the study of pore pressure responses in grouted piezometers and the pore pressure buildup in areas with rainfall-induced landslides failures. This phenomenon of pore pressure diffusion is coupled with Terzaghi's theory of consolidation. For that purpose, an analysis of pulse tests (consisting of measuring pore pressure response with time due to increases in pore water pressure boundary conditions) conducted by previous researchers is performed. In conjunction with the pulse tests, modified consolidation tests are also executed. The coefficients of diffusion affecting the pore pressure response in each of these cases are then evaluated.

In addition, an analytical model is developed to mathematically describe the pore pressure response in clays under pressure pulses. The derivation of the differential equation describing this response makes use of Darcy's theory of flow in porous media, where a difference in gradients causes a difference in flow patterns. The derived equation is then compared to Terzaghi's equation of consolidation. This couples model shows that a sudden pulse of pressure causes a slower pore pressure response than the one caused by an increase of total stress.

The role that pore pressure diffusion and consolidation simultaneously contribute are studied in a modified CRS consolidation setup. The mathematical modeling of these processes together is compared to the experimental results. Due to these two processes working together, at

no particular point in time is there an increase of pressure at any depth in the soil that matches the initial increase of pressure application.

The research also mentions the limitations of applying the derived equations. These limitations are inherently related to the simplifying assumptions presented in the theory, as well as to the complexity of porous media. Future follow-up research is also suggested.

Table of Contents

Table of figures

Table of tables

1 INTRODUCTION

The most agreed upon definition of a porous medium is one that has interstitial pores whose size allows other smaller molecules to penetrate though a diffusion mechanism. It should have a specific permeability, the value of which is a function of the properties of the pore geometry, not of the properties of the diffused fluid.

The role that flow in porous media plays has been studied in numerous fields. In petroleum engineering, the processes of well drilling and extraction of oil depend on the properties of porous media. In chemical engineering, the study of heterogeneous catalysis, where reactants (usually gases) diffuse to the catalyst surface and adsorb onto it, depends on the properties of the porous structure. In geotechnical engineering, water flowing through porous media in the vicinity of engineered structures results in changes in pore pressures. These pressures, coupled with deformation, cause changes in the effects of mechanical loading and therefore can influence the stability of the structure through its interaction with the soil. The study of these coupled effects has been driven by the need to understand the "consolidation" processes happening due to applied pressures on soils (Terzaghi and Biot). The role of pore fluid has since been expanded to several other applications, such as failure induced by pressurization of a borehole, hydraulic fracturing and propagation of fractures in earthquake mechanics, to name a few.

This thesis focuses on better understanding the pore pressure diffusion processes happening in high plasticity clays. The real-life application that it intends to address is pore water pressure monitoring in areas prone to landslides, in particular landslides triggered by brief and intense rainfall. These happen due to locally elevated pressures along the failure surface. Infiltration of water is due to multi-dimensional pressure diffusion problem best estimated by a non-linear form of Richard's equation, where variations in pressure head are a function of changes in hydraulic conductivity and volumetric water content (Reid, 1994). This paper takes a look at this process in saturated soil, which is a good assumption to make in areas where rainfall is intense and over a short period of time. Baum and Reid (1995) discovered that surface infiltration in these conditions can saturate a body of soil in just a few days. The problem can be simplified by looking at one-dimensional linear diffusion models to get a transient fluctuation response of pressure with depth. In this thesis, results from modified 1-D consolidation tests were analyzed to better understand pore pressure propagation though soils. The modified consolidation tests included measuring the

pore pressure buildup and dissipation at the base of a specimen while the total stress or pore pressure at the surface were changed. The volumetric changes were recorded over time as well to provide an independent measure of consolidation.

Following this introductory Chapter 1, the thesis is composed of the following six chapters:

- Chapter 2 provides a literature review of porous media and the pore pressure diffusion happening in these media. These processes are examined in conjunction with their dependency on soil properties. The background theory on pressure diffusion (outlined in Biot's and Terzaghi's research) is also presented, along with simple linear diffusion model and possible applications in real life.
- Chapter 3 presents an analytical model of pore pressure propagation that best simulates the pore pressure response in clays due to a pulse of water at its top boundary. The analysis discusses the gradients associated with the boundary conditions adopted and the derivation of the differential equation of the flow caused by the difference in gradients with depth.
- Chapter 4 is an outline of the experimental procedure used by previous researchers to obtain the data that is analyzed in this study. The tests used in the analysis consist of consolidation tests and "pulse" tests, the difference between which is associated with different sets of boundary conditions.
- Chapter 5 outlines the analysis and modeling of the experimental results. The consolidation and pulse tests results are compared in terms of time response due to change in pore pressure, as well as the difference in the corresponding diffusion coefficients.
- Chapter 6 highlights the main conclusions from this research and lists future follow up research to continue this work.

2 LITERATURE REVIEW

2.1 Introduction to porous media

This section of the literature review presents a brief overview of the basic concepts that are relevant to understanding behavior of porous media and the flow and water propagation through it.

2.1.1 Definition of a porous medium

A porous medium is defined as a solid with uniformly distributed voids throughout the bulk. The "matrix" is the skeletal portion of the medium, which refers to the solid phase. The pores are filled with a fluid (gas and/or liquid). Many natural materials (soil and rock) and man-made substances (concrete, ceramics) can be considered to be porous media. The pores in the matrix can either be continuous or non-continuous. A visualization of a porous medium is presented in Figure 1.

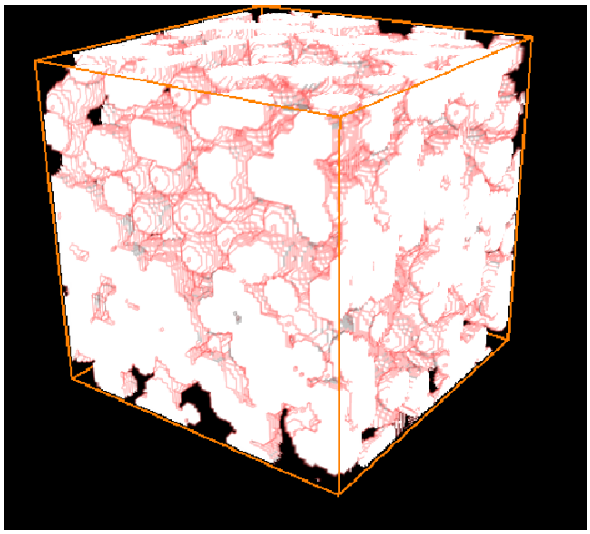

Figure 1 Digitalized porous medium built from overlapping randomly placed spheres (https://ciks.cbt.nist.gov/~garbocz/reldiff/node4.html)

Porous materials have different mechanical behaviors from non-porous ones, so their identification is usually done by performing experiments on a sample, such as density and yield strength. Such sets of experimental procedures are important characterization tools in a numbers of scientific and engineering branches. (Dullien, 1991).

Two approaches can be adopted in the study of porous media: (Lancellotta, 2002)

- The microscopic approach: each phase constituting the porous medium is studied on its own as a single body using a micromechanical approach. The interaction mechanisms at the interfaces of these individual bodies also have to be taken into account to get a complete understanding of the multiphasic medium.
- The macroscopic approach: it uses a homogenization method, where the different phases are distributed through the body using an averaging process.

The two approaches have an ultimate goal of identifying macroscopic properties of the medium. Both approaches have been studied in the literature (Dullien, 1991 and Ehlers, 2002) and have their own advantages and merits in different areas of research. The microscopic approach is used in atomic and molecular physics for studying the atomic or molecular structure of the different phases and their interaction. This method has an advantage of describing the individual elements of the body based on their own motion, considering the well-studied separate characteristics of each phase. However, one major difficulty arises from determining the coupling mechanisms of the phases at their interface. One other difficulty is the fact that the detailed geometry and distribution of pores on the microscopic level is almost impossible to characterize. In addition, no two similar specimens will have the same pore distribution. For this reason, in most other areas of engineering, the macroscopic approach presents a more practical approach. It is easier and more practical to focus on the macroscopic analysis of features that are assumed to be independent of the pore configuration. Making this assumption has the advantage of making the description repeatable and predictable.

In the following discussions, a macroscopic approach based on the theory of mixtures and the concept of volume fraction is going to be used.

2.1.2 Porosity

Porosity is one the basic characteristics of a porous medium. By definition, porosity is the fraction of the volume of the medium that is occupied by void space, or "pores". Equation 1 represents this relationship:

$$\varphi = \frac{V_v}{V_t} = 1 - \frac{V_s}{V_t} \qquad \text{(Equation 1)}$$

Where φ is the porosity (a number from 0 to 1)

V_v is the volume of the voids [L^3]

V_s is the volume of solids [L^3]

V_t is the bulk volume, or total volume of the material [L^3]

Over the course of sediment deposition, some void spaces become isolated from each other due to excess cementation. This geologic occurrence makes it important to differentiate between "interconnected" and "isolated" pore spaces. Figure 2 shows the difference between those two different types.

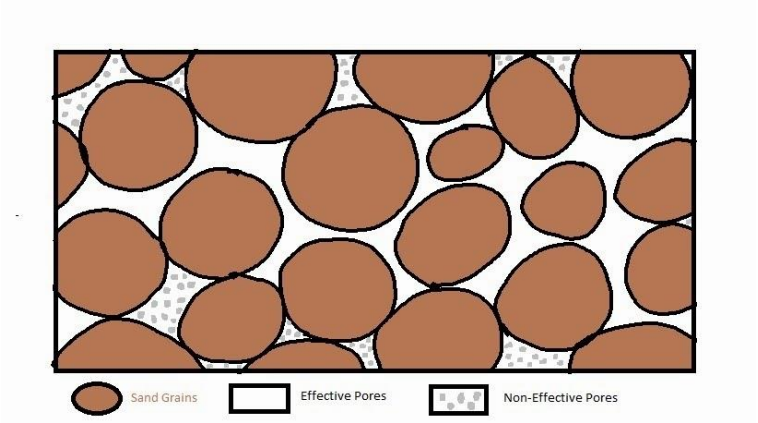

Figure 2 Illustration of pores and effective pores in a sand porous medium (Reservoir Engineering Online, 2014)

This leads to two different values of porosity:

- Absolute porosity, which indicates the total volume of voids in the medium as a function of the total volume. This includes both interconnected and isolated pores.
- Effective porosity, where the fraction of only interconnected pores is of interest.

From the point of view of flow in porous media, the effective porosity is the one that is more important. In fact, a material can have a high absolute porosity, yet may not conduct much fluid due to a lack of interconnected pores. For granular materials and poorly to moderately cemented soils, the effective porosity is close to the absolute porosity. For heavily cemented clays, there can be a significant difference between the two (Katsube, 2010).

2.1.3 Hydraulic conductivity

Hydraulic conductivity is another very important parameters that affects the pore water pressure response in a porous medium. Also known as "permeability", it is defined as the capability of the soil to transmit water when subjected to a hydraulic gradient.

Hydraulic conductivity is defined according to Darcy's law, which relates the fluid flux to the change in gradient:

$$q = -ki \qquad \text{(Equation 2)}$$

where q is flux [L/T]

k is hydraulic conductivity [L/T]

i is gradient [L/L]

Hydraulic conductivity depends on several factors in the soil, including pore size distribution, fluid viscosity, grain size distribution, void ratio, specific area of solids and degree of saturation. The last two factors make the most difference as to how high k would be: the higher the surface area, the lower the value of k (as is the case in clays); the higher the degree of saturation, the higher the value of k. In fact, k assumes a maximum value when the soil is fully saturated.

The estimation of k can be determined by two different ways:

- Experimentally, by performing a constant head test or a falling head test. Both techniques consist of confining the ends of a sample in a hydraulic conductivity ring with plates that contain porous stones. This ensures constant volume throughout the test procedure. A better control over the stress in the cell can be achieved by placing the specimen in a consolidation cell with a suitable loading frame. In any case, the sample is hooked up with an inflow valve and an outflow valve. A change in gradient happens due to water inflow and the time needed for the water to get out of the specimen through the outflow valve is measured.

  In the constant head test, the hydraulic gradient is kept constant and the hydraulic conductivity is calculated as follows:

$$k = \frac{QL}{H_l A t} \qquad \text{(Equation 3)}$$

Where Q is the flow of fluid (L^3)

L the length of the specimen

H_l the head loss across the specimen

A the cross-sectional area of the sample

t the time over which Q is measured

In the falling head test, the hydraulic head decreases with time. If the head loss at a time t_1 is H_1, and at time t_2 is H_2, and if the cross-sectional area of the burette where the water is falling is a, then

$$k = \frac{aL}{A(t_2 - t_1)} \ln\left(\frac{H_1}{H_2}\right) \qquad \text{(Equation 4)}$$

- By using analytical correlations. For example, if a consolidation test is being conducted, then the hydraulic conductivity can be back-calculated from the coefficient of consolidation:

$$k = c_v m_v \gamma \qquad \text{(Equation 5)}$$

Where m_v is the coefficient of compressibility

c_v the coefficient of consolidation

γ the unit weight of the fluid

More information on consolidation is presented in later sections.

2.1.4 Biot's theory of poroelasticity

The presence of water in a poroeslastic medium changes its mechanical properties, a theory that has been adopted and analyzed by several researchers in different fields. This change in behavior is summarized by two observations (Detournay & H.-D. Cheng, 1993):

- An increase in pore pressure dilates the medium
- If fluid is prevented from escaping, a compression causes a rise in pore water pressure

The coupling of deformation-diffusion mechanisms has been addressed by several theories, including Terzaghi's theory of one-dimensional consolidation. However, it was Biot in 1941 who developed a linear theory of poroelasticity that described both mechanisms mentioned above. Biot

later expanded his own theory to include wave propagation of diffusion waves in porous media. The importance of providing a brief discussion of Biot's theory in this paper lies with the fact that the definitions of compressibility provided by it are applicable to the pore pressure diffusion problem.

Biot introduced a quantity that he named "the increment of fluid content" ζ, which describes the "volume of the water exchanged by flow into or out of the control volume". To put it in another way, it represents the amount of water stored in the system. The keys concepts in Biot's theory are represented by two main constitutive equations:

$$\epsilon = a_{11}\sigma + a_{12}p \qquad \text{(Equation 6)}$$

$$\zeta = a_{21}\sigma + a_{22}p \qquad \text{(Equation 7)}$$

where ε is the volumetric strain, positive in expansion, negative in contraction

σ is the applied stress, positive in tension, negative in compression

p is the pore pressure

The terms a_{11}, a_{12}, a_{21} and a_{22} are poroelastic constants which can best be described as the change in a dependent variable relative to a change in an independent variable. They are defined as follows:

$$a_{11} = \left.\frac{\delta\epsilon}{\delta\sigma}\right|_{p=0} \equiv \frac{1}{K} \qquad \text{(Equation 8)}$$

$$a_{12} = \left.\frac{\delta\epsilon}{\delta p}\right|_{\sigma=0} \equiv \frac{1}{H} \qquad \text{(Equation 9)}$$

$$a_{21} = \left.\frac{\delta\zeta}{\delta\sigma}\right|_{p=0} \equiv \frac{1}{H_1} \qquad \text{(Equation 10)}$$

$$a_{22} = \left.\frac{\delta\zeta}{\delta p}\right|_{\sigma=0} \equiv \frac{1}{R} \qquad \text{(Equation 11)}$$

where K is the drained bulk modulus

$1/H = 1/H_1$ is the poroelastic expansion coefficient

R is a poroelastic constant, 1/R is called specific storage coefficient

The term 1/K is called drained compressibility, and it accounts for both the fluid and the solid matrix. It is therefore related to the change in porosity.

Other constants, such as Skempton's coefficient, can also be derived from the three originally defined parameters. The definition of Biot's compressibility is important to the solution of the diffusion problem, as it was the first one that related the bulk modulus to the variation of water content in the soil, and therefore the pore pressure response due to applied pressure. In addition, Biot's theory made other derivations regarding drained and undrained response possible in diffusion problems.

2.2 Fluid diffusion

The phenomenon of pore pressure diffusion occurs due to the behavior of flowing water. Water molecules that traverse a solid mass of clay adheres onto the interlayer of clay minerals, forming a film. This process is called "adsorption" and water can be classified into two categories of adsorption (Tang, Chen, & Song, 2016):

- Strongly adsorbed water: has a solid-like structure and can therefore be considered a part of the solid phase. Cannot participate in the process of diffusion
- Loosely adsorbed water: is not fixed and therefore can participate in laminar flow. As long as there is loosely adsorbed water, the propagation of water from a point to another in ac clay sample can happen.

These definitions apply only to clay minerals, as they have a large surface area and a negative charge on their interface, which permit the water molecules to get adsorbed. For this reason, water propagation in granular materials follows a very different scheme that in clays.

A parameter called "loosely adsorbed index" I_{lo} defines the content of loosely adsorbed water present in a clay material. If $I_{lo} > 1$, loosely adsorbed water practically behaves like free water. When $I_{lo} \rightarrow 0$, the properties of the water change to a more strongly adsorbed state.

When an excess pressure is applied, the amount of free water and loosely adsorbed water decrease. I_{lo} decreases in the process, producing a slower response rate. This causes a "time-lag effect" that gives the pore pressure distribution its known asymptotic shape. Tang et al. (2016) conducted a series of laboratory tests where samples of clay were subjected to water pressure increases at the top after isotropic consolidation and the pore pressure response at the bottom of

the specimens was measured with time. They found that if the only parameter that is changing between different sets of tests is the water pressure input, the pressure response due to diffusion is very consistent over time. As seen in Figure 3, as the consolidation pressure decreases, there is more free water in the clay, which allows for the diffusion to propagate at a faster rate.

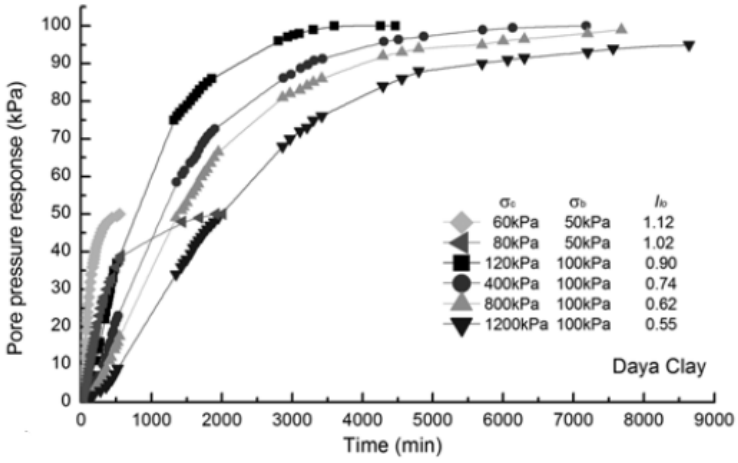

Figure 3 Pore pressure responses in diffusion tests in consolidated clay, with a consolidation pressure between 60 and 1200 kPa

2.2.1 Diffusivity

The diffusion coefficient ***D*** (or diffusivity) is a parameter indicative of the diffusion mobility. The definition of the diffusion coefficient arises from Fick's law of diffusion. This law relates the diffusive flux to concentration in steady-state conditions. The postulation behind this theory is that flux goes from regions of high concentration to regions of low concentration. This can be applied to a series of experimental observations, from solids to liquids to gases. In particular, Fick's second law of diffusion describes how the change in concentration occurs with time.

For diffusion of liquids through porous media, D is referred to as hydraulic diffusivity. Equation 12 is the definition of D, derived from Richard's equation combined with Darcy's law (Berti & Simoni, 2010).

$$D = \frac{k(\Psi)}{C(\Psi)} = \frac{k(\Psi)}{\frac{d\theta}{d\Psi}} \qquad \text{(Equation 12)}$$

where k(Ψ) is the hydraulic conductivity [L/T]

C(Ψ) is the specific moisture capacity

θ is the volumetric water content

Ψ is the pressure head

K and C heavily depend on the degree of saturation of the medium. In case of complete saturation, the equation for D becomes:

$$D_{sat} = \frac{k_{sat}}{C_0} \qquad \text{(Equation 13)}$$

where K_{sat} is the saturated hydraulic conductivity

C_0 is the specific moisture content at saturation

The value of K_{sat} can be obtained by performing a constant head or falling head test on a clay specimen that has been back-pressured to saturation. The specific moisture content at saturation C_0 can be obtained by performing a series of odometer tests. The odometer modulus ($\Delta\sigma'_v/\Delta\varepsilon_v$) relates the vertical deformation $\Delta\varepsilon_v$ (compression) with a change in stress $\Delta\sigma'_v$. Specific moisture content is itself connected to the compressibility of the soil, and therefore the relationship between vertical deformation and volumetric water content can lead to the determination of C_0.

Treating D as a constant during saturation makes the diffusion model linear, and therefore easier to solve. The use of D_{sat} is reasonable enough when dealing with mechanisms that trigger a significant increase in pore water pressure such as rainstorms, especially ones that trigger failure (Reid, 1994). Scenarios of unsaturated media are discussed later in this section.

Through correlations, Equation 13 for D can be expressed as follows (Yang, Li, & Zhang, 2015):

$$D = \frac{K}{\varphi\beta\mu} \qquad \text{(Equation 14)}$$

where K is the permeability [L^2]

φ is the porosity

β is the compressibility [psi^{-1}]

μ is the fluid viscosity [psi.sec]

The permeability K is related to the hydraulic conductivity k by the following relation:

$$K = k\frac{\mu}{\gamma} \qquad \text{(Equation 15)}$$

2.2.2 Simple linear diffusion model

Pore pressure diffusion waves happen when a classical diffusion equation is paired with an oscillatory function. For simplicity, the pressure diffusion wave propagation will be analyzed in a one-dimensional, homogeneous, isotropic and saturated medium.

The pressure (P) as a function of distance x and time t, diffusion equation is given:

$$\frac{\partial u(x,t)}{\partial t} = D\frac{\partial^2 u(x,t)}{\partial x^2} \qquad \text{(Equation 16)}$$

The boundary conditions adopted to solve this equation are:

$$t = 0,\ x > 0,\ u = 0$$
$$t > 0,\ x = 0,\ u(0,t) = u_0$$
$$t > 0,\ x = \infty,\ u(\infty,t) = 0$$

The solution is presented in the form of a Laplace transform harmonic wave equation. By applying a Fourier transform, the equation can be solved with this form of solution

$$u = \bar{u}\left[1 - \text{erf}\left(\frac{z}{2\sqrt{Dt}}\right)\right] \qquad \text{(Equation 17)}$$

where u is the pressure at depth z and time t

and D is the coefficient of diffusivity as defined in Section 2.2.1.

The pressure gradient is therefore:

$$\frac{\delta u}{\delta z} = \bar{u}\left[-\frac{1}{\sqrt{\pi}\sqrt{Dt}}e^{-\frac{z^2}{4Dt}}\right] \qquad \text{(Equation 18)}$$

The function is asymptotic with time (note the decrease in $\delta u/\delta z$ with time).

Yang and Li have studied the effect of the change of the water properties and the frequency of diffusion waves on the equation parameters. The paper discusses the effect of frequency on all the above parameters, for specific values of permeability.

The behavior of pressure waves can be summarized as below:

- When permeability decreases, wave velocity peaks occurs at higher frequencies.
- As frequency increases, wavelength and penetration depth of the pressure wave decrease.
- When permeability decreases, the peak wavelength and the peak penetration depth both shift toward low frequencies.
- When frequency is low, there is enough time for the wave to come to equilibrium

Figures 4 through 6 show spatial-temporal distribution of pressure diffusion waves in porous media.

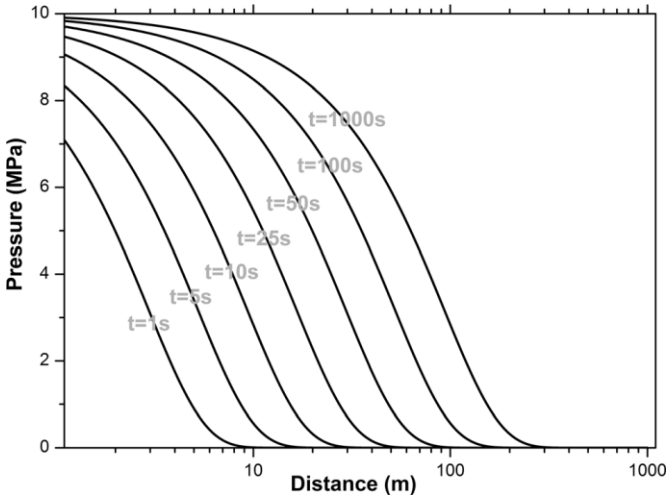

Figure 4 Pressure diffusion versus distance for different travel times

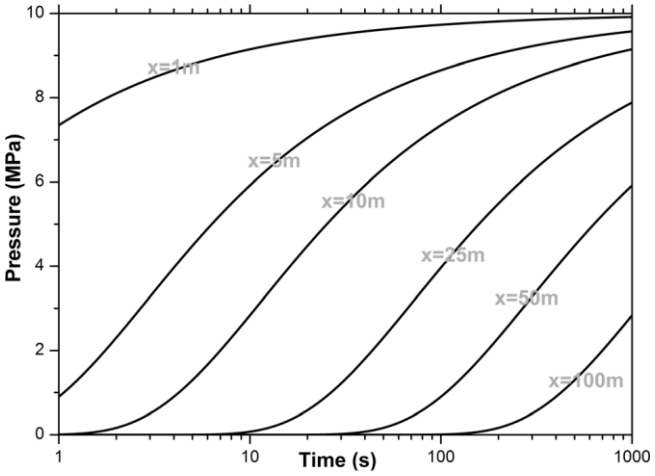

Figure 5 Pressure as a function of travel time for various propagation distances

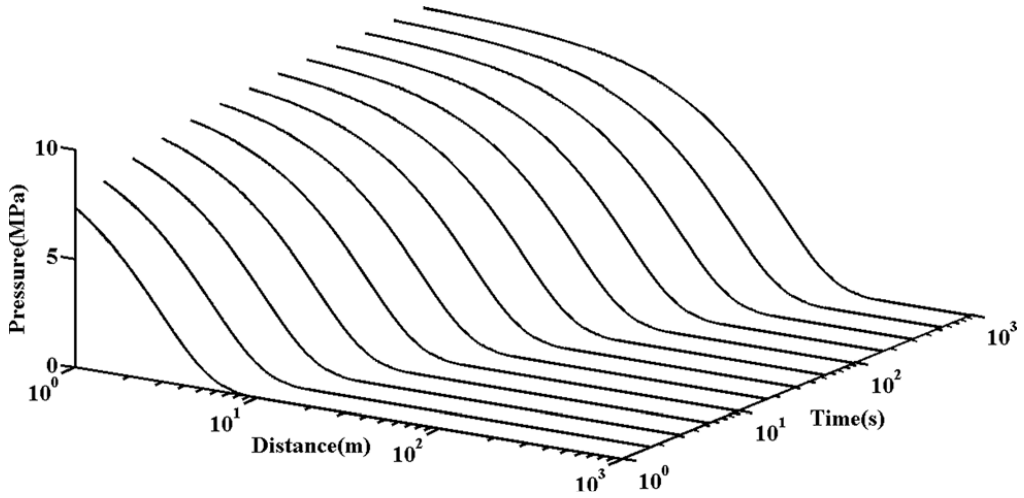

Figure 6 Spatial and temporal distribution of pressure

Figure 6 shows the variation of the pressure with distance for several travel times. For a given time, pressure decreases as distance increases. Figure 7 shows the pressure profile vs time for several depths of reach, and Figure 6 shows both the space and time dependencies of the pressure. As seen in Figure 5 and Figure 6, there is a time lag until any pressure change is detectable at a specific distance. The speed of propagation of the diffusion waves is very high, but the amplitude of the waves decreases with distances, which is the reason for the time lag and the decreasing pressure values.

Although not discussed in this document in any further detail, it is worth to mention that when travelling through heterogeneously varying soils in terms of diffusivity, the pressure diffusion waves are accelerated and amplified when crossing through an interface leading to a higher diffusivity soil.

2.3 Terzaghi's theory of consolidation

Terzaghi's theory of consolidation is a specific case of pore pressure propagation where a saturated clay is loaded externally. The water is squeezed out of the soil over a period of time. This leads to vertical deformations (settlements), which could range from instantaneously for granular materials to over several years for clays. The deformation of saturated soil occurs by reduction in pore space.

If a surcharge q is subjected to the top of a clay specimen, there is an instantaneous increase in stresses across the soil, equal to q. These stresses are first acquired by the water: the pore water pressure Δu increases initially by q. As the water gets expelled through one or two boundaries, this increase in pressure gets transferred from the water to the solid particles, resulting in an increase in effective stress over time, as can be seen in Figure 7.

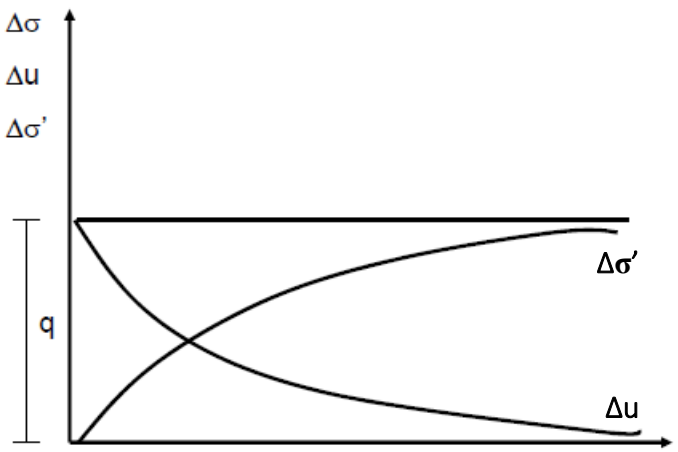

Figure 7 Change in excess pore pressure and effective pressure during consolidation

Terzaghi's consolidation is isotropic and one-dimensional, which means that drainage and deformations are vertical (which is a reasonable simplification if the surcharge is of a large extent).

The diffusion coefficient in Terzaghi's formulation is called "coefficient of consolidation" and the propagation of water is represented by the following differential equation (Equation 19):

$$\frac{\partial \bar{u}}{\partial t} = c_v \frac{\partial^2 u}{\partial z^2} \qquad \text{(Equation 19)}$$

Where $\bar{u}$ is the excess pore water pressure

t is time

z is depth

The solution to this equation is

$$\bar{u} = \sum_{m=0}^{\infty} \frac{2\bar{u}_i}{M} \sin\left(\frac{Mz}{H}\right) e^{-M^2 T} \qquad \text{(Equation 20)}$$

Where

$$M = \frac{\pi}{2}(2m+1) \qquad \text{(Equation 21)}$$

and

$$T_v = \frac{c_v t}{H_{dr}^2} \qquad \text{(Equation 22)}$$

The term H_{dr} is the longest drainage path of the escaping water. In one-way drainage situations, it is equal to the entire length of the soil block.

An average degree of consolidation U can be derived from this expression:

$$U = 1 - \sum_{m=0}^{\infty} \frac{2}{M^2} e^{-M^2 T} \qquad \text{(Equation 23)}$$

Hansen (1961) derived a good approximation for U as a function of T_v:

$$U = \left(\frac{T_v^3}{T_v^3 + 0.5} \right)^{1/6} \qquad \text{(Equation 24)}$$

2.4 Current empirical literature about pressure propagation in porous media

Several studies have looked into the application of pore pressure diffusion theory into real-life situations. Two of the most notable examples of such applications are the study of pore pressure propagation in landslide prone areas, and in liquefaction situations.

Berti et al. (2010) looked at the processes related to pore pressure diffusion in areas prone to landlsiding and proposed a simple linear diffusion model that would predict the groundwater response in a flow body subjected to rainfall. Assumptions that are deemed reasonable were made in the process. For example, the soil was considered to be saturated. In fact, this can be considered true in particular situations. Baum and Reid (2005) discovered that surface infiltration can saturate the landslide body in just a few days, and that the saturated soil responds rapidly to heavy rainfall. In a sloping area, the response of a semi-infinite slope to rainfall is theoretically given by:

$$\frac{\partial \Psi}{\partial t} = D_0 cos^2 \alpha \frac{\partial^2 \Psi}{\partial Z^2} \qquad \text{(Equation 25)}$$

where Z is the vertical depth from the ground surface and α is the slope angle.

This theoretical model was compared to actual collected data using piezometers installed at several locations underneath the surface. The recorded measurements (Ψ^{obs}) were compared with the simulated data (Ψ^{obs}) using the following procedure:

- Choosing a trial value of D_0

- Computing the pressure heads with the above equation, with the recorded rainfall as the upper boundary and a constant saturated hydraulic conductivity
- Evaluating how the calculated numbers Ψ^{sim} fit to the data Ψ^{obs} using the Nash-Sutcliffe efficiency coefficient:

$$E_f = 1 - \frac{\sum_{n=1}^{N}\left(\Psi_n^{obs} - \Psi_n^{sim}\right)^2}{\sum_{n=1}^{N}\left(\Psi_n^{obs} - \overline{\Psi^{obs}}\right)^2} \qquad \text{(Equation 26)}$$

  A value of E_f of -∞ is the worst match, and 1 is a perfect match.

- Evaluating the calibrated value of D_0 using an algorithm to converge the value of E_f to a maximum.

The theoretical model and the observed data agreed well with one another, as long as the assumptions used in the model are not violated. Results can be seen in Figure 8.

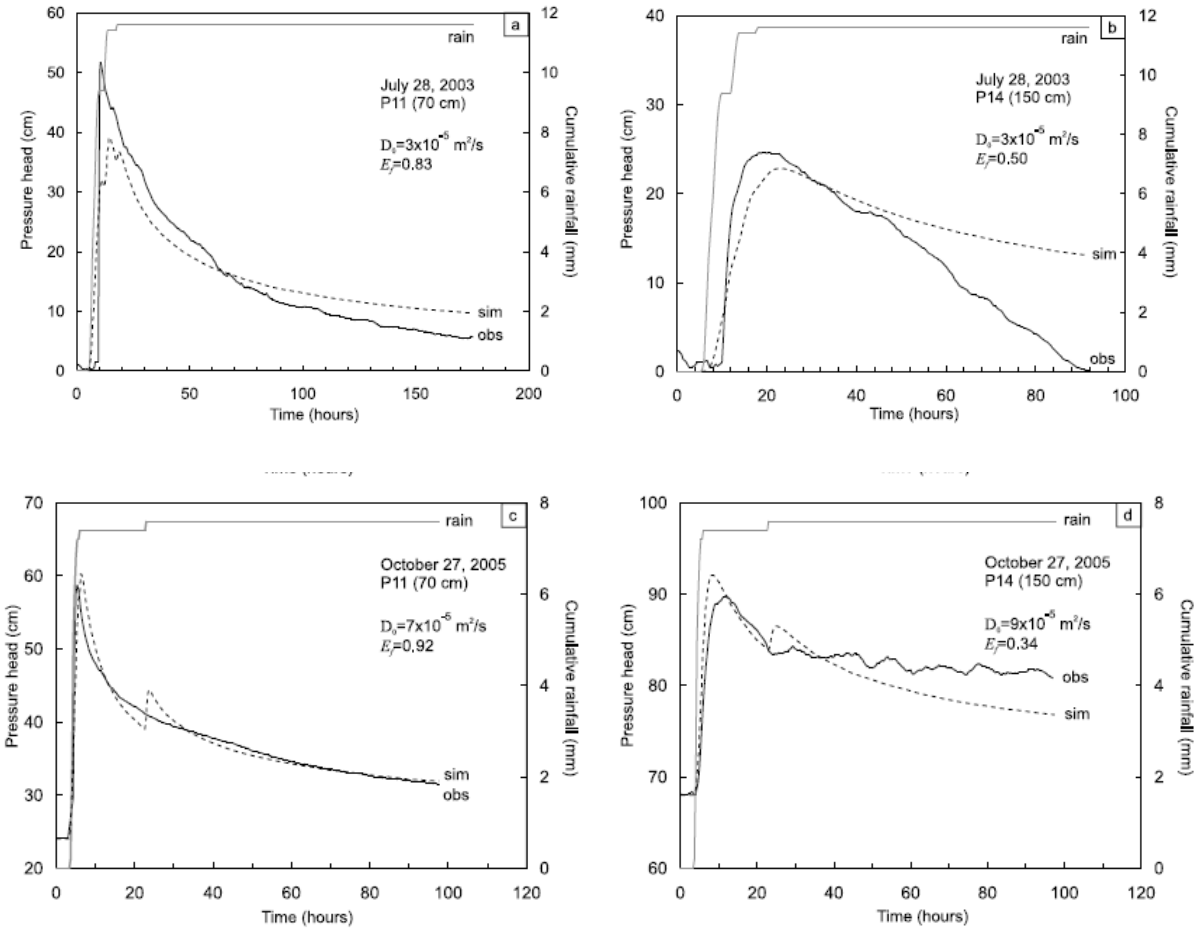

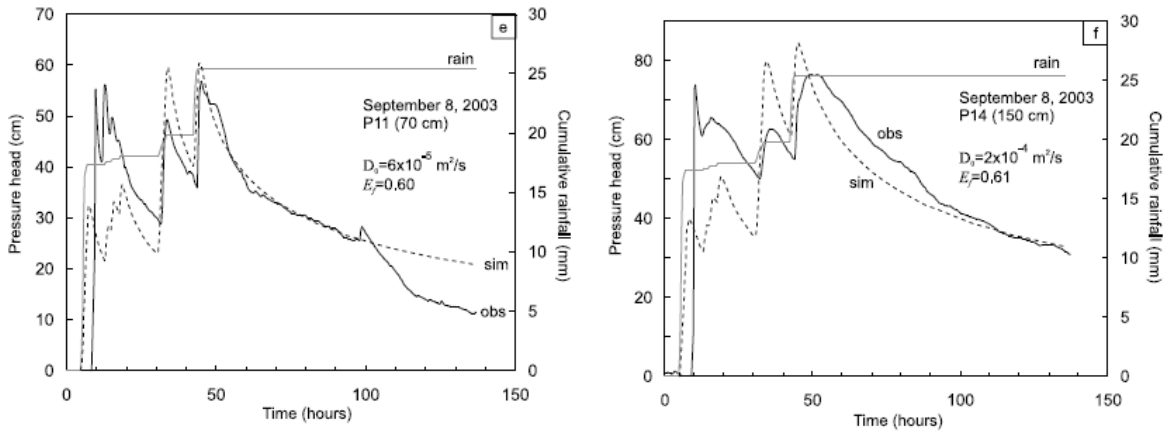

Figure 8 Comparison of observed (pbs) and simulated (sim) pore pressure response to rainfall

The increase in pressure head and the time lag to peak are also similar to what is observed in the field, as seen in Figure 9.

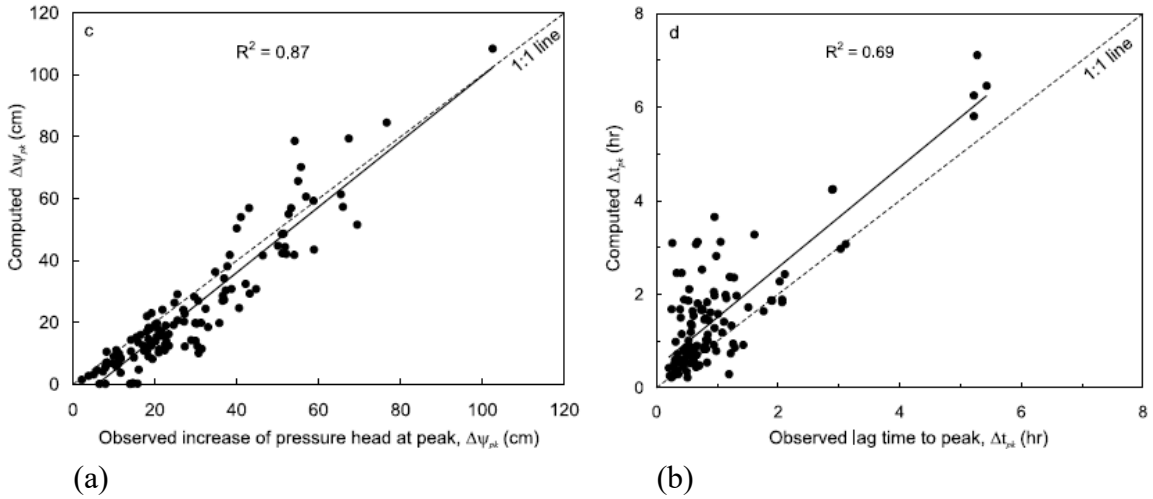

Figure 9 Comparison between observed and computed increase of (a) pore pressure at peak and (b) time lag to peak

Possible examples of violation happen:

- in the wet season, when ponding happens to high precipitation (the soil is at saturation). In such case, the infiltration rate becomes less than the rainfall intensity.
- if the surface soil is unsaturated: the model works best in saturated conditions

An important note to make about the basal boundary condition is that the measurements of hydraulic conductivity K of the bedrock show that it is less than the overlying clay cover. This

means that there should have been a ponding at the top of the bedrock. However, measurements show that pore pressure data can be reproduced with a constant basal boundary condition. To investigate this, 3 hydrologic models were proposed:

- One with a homogenous slope ($K_{bedrock} = K_{cover}$)
- One where the hydraulic conductivity of the bedrock is much less than that of the clay
- One intermediate state with a partially leaking bedrock ($K_{bedrock} \approx 0.1\ K_{cover}$)

The results of these models at a distance in the cover and at the bedrock are shown in Figure 10.

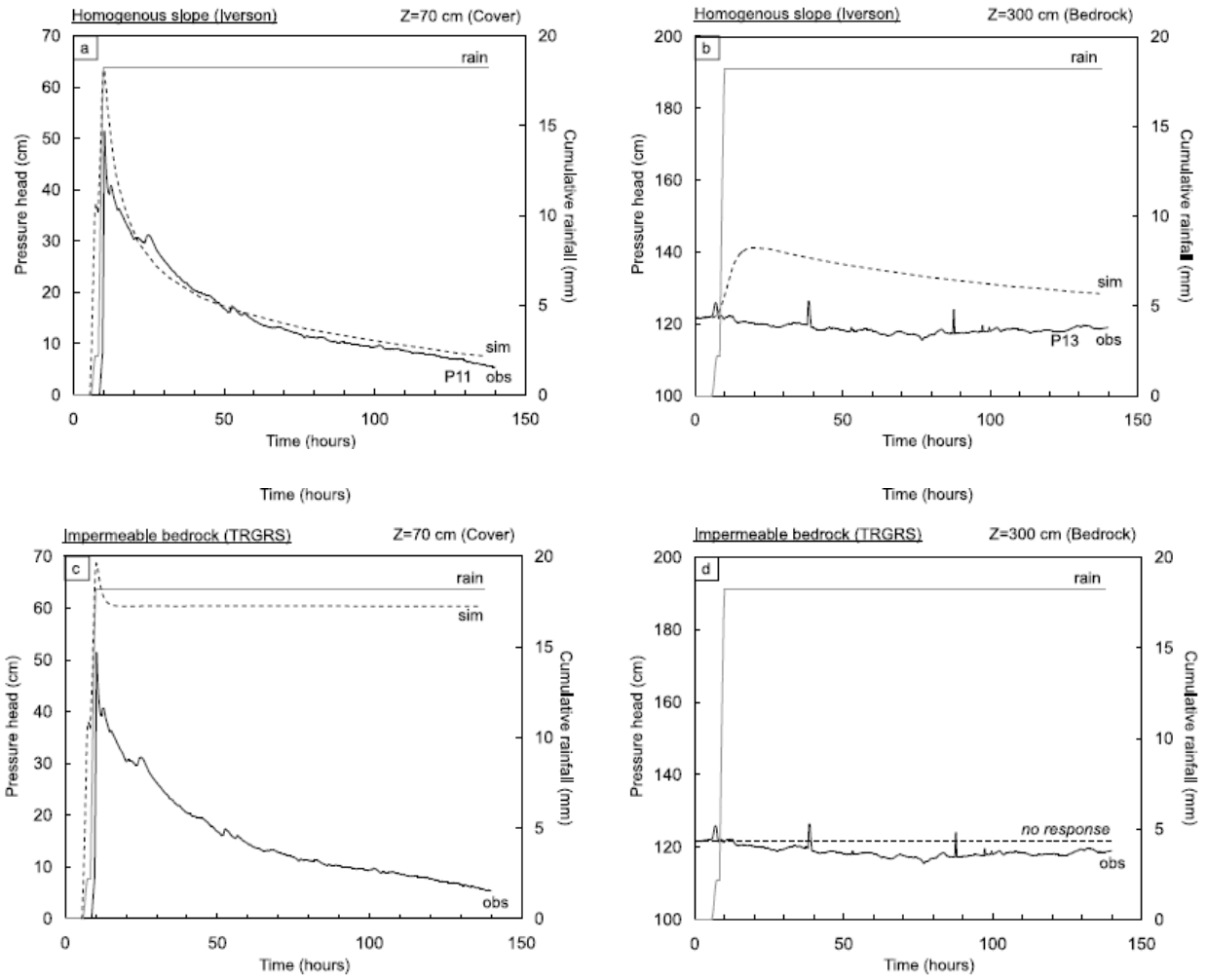

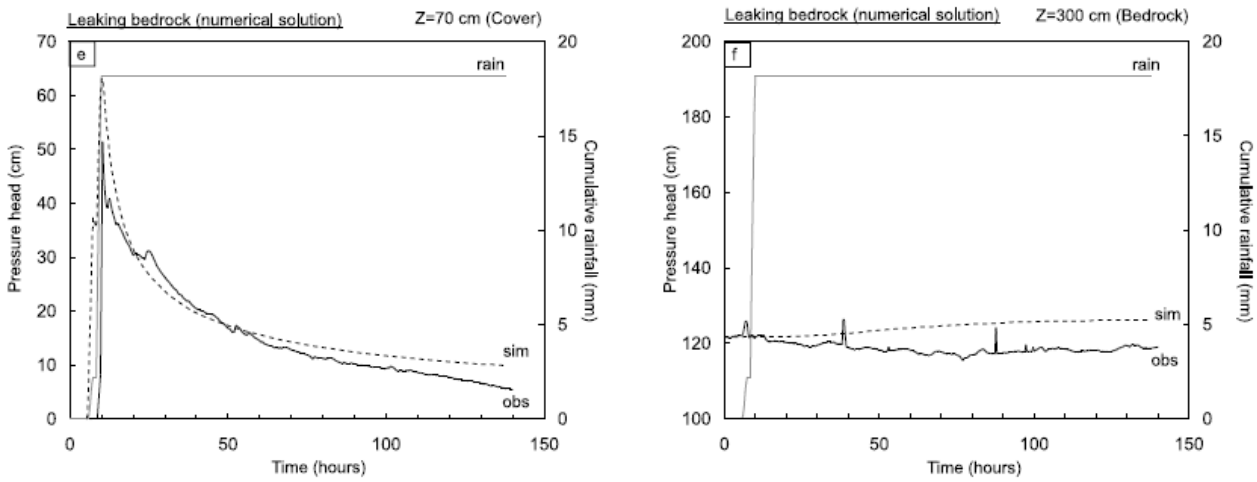

Figure 10 Comparison of observed and computed pore pressure response to rainfall for 3 different hydrologic models

The best model that fits observed data is the 3rd one: partially leaking bedrock. The 2nd model predicts accumulation of water at the bottom of the cover, which wasn't observed in the field. One reason for this may be the existence of a fissure network which allows water to reach the bedrock.

The observations regarding hydraulic conductivity show that the use of a linear diffusion model is limited by the uncertainty that affects the hydraulic parameters. For landslide susceptibility analysis, it is not recommended to use a theoretical model without proper support from data in the field.

3 ANALYTICAL MODEL OF PORE PRESSURE PROPAGATION

3.1 Assumptions

The assumptions used in formulating this theoretical model as very similar to those proposed by Terzaghi in his consolidation theory.

1. The soil is homogeneous and isotropic.
2. The soil is saturated.
3. The solid and water elements are incompressible.
4. Darcy's law is valid
5. Flow and compression are one-dimensional (vertical)
6. All strains are relatively small
7. Soil properties are constant

3.2 Pulse test model

The propagation of water in a clay specimen caused by a pulse of water at the top can be reproduced in the laboratory by conducting a series of "pulse" tests. A pulse test is performed by increasing the pore water pressure at the top of a clay specimen in a consolidation cell. Then, the pressure equalization vs. time is measured at the bottom of the specimen under one-way drainage conditions. The difference between the pore pressure changes with time in a pulse test versus in a typical consolidation test is due to the initial and boundary conditions involved in the two tests.

In a consolidation test, the total load is increased at time 0; it is assumed that this change will result in an increase in pore water pressure across the clay height right after application of the load. Due to the expulsion of water that occurs over time, the pore water pressure decreases and the effective stress increases. In a pulse test, the pore water pressure is increased at the top only. At time 0, there is no increase in pore pressure at any other point in the clay, as opposed to what supposedly happens in a consolidation test.

The boundary and initial conditions in each of these two scenarios are displayed in Figure 11.

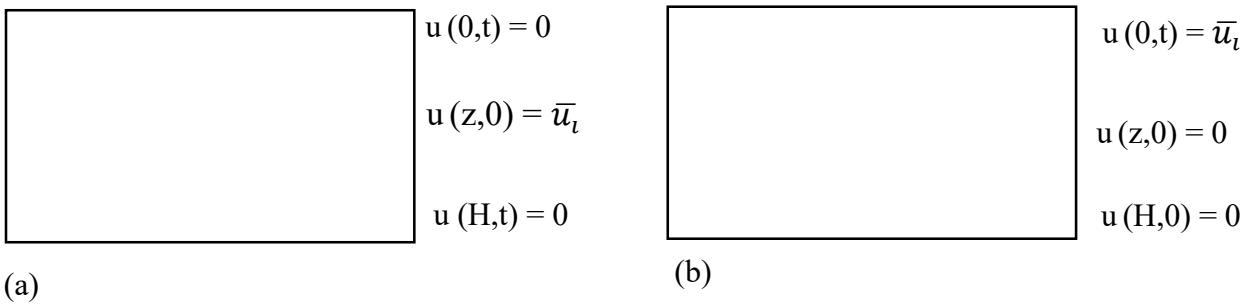

Figure 11 Initial and boundary conditions for (a) a typical consolidation test with double drainage (b) a pulse test shown on a clay sample of height H

$\bar{u}_i$ is the increase in pore water pressure at time 0.

The previous discussion implies that pore pressure pulses migrate in a specimen under different gradients than in consolidation. Assuming Darcian flow, a different gradient will result in a different flow pattern and therefore a different propagation scheme. Darcy's law states that:

$$Q = -kiA \qquad \text{(Equation 27)}$$

where Q is the discharge (in units on [L/T^3]), k is the hydraulic conductivity [L/T], i is the gradient [L/L] and A the area [L^2].

The unit discharge q (discharge/unit area) is therefore defined as in Equation 2 presented in Section 2.1.3:

$$q = -ki$$

By definition, the gradient i, which drives the flow, is the rate of head change over the distance that the fluid travels. For a strip of clay with height dz, an annotated schematic of which is shown in Figure 12, the gradient i is determined following Equation 28.

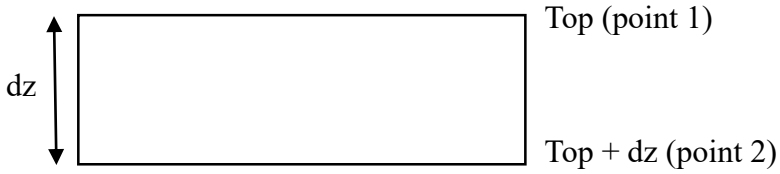

Figure 12 Infinitesimal element of soil under study

$$i = \frac{\partial h}{\partial z} = \frac{\partial \left(z + \left[\frac{u_{hyd} + u_e}{\gamma} \right] \right)}{\partial z} \quad \text{(Equation 28)}$$

where h is the total head

u_{hyd} is the hydrostatic pore water pressure

u_e is the excess pore water pressure at the time of application

γ_w is the unit weight of water

The excess pore water pressure is the one that drives the water flow. Equation 28 reduces to:

$$i = \frac{1}{\gamma} \frac{\partial \bar{u}}{\partial z} \quad \text{(Equation 29)}$$

The head gradient at point 1 is:

$$i_1 = \frac{1}{\gamma_w} \frac{\partial \bar{u}}{\partial z} \quad \text{(Equation 30)}$$

The head gradient at point 2 is:

$$i_2 = \frac{1}{\gamma_w} \frac{\partial}{\partial z} \left(\mathbf{0} + \frac{\partial \bar{u}}{\partial z} dz \right) = \frac{1}{\gamma_w} \frac{\partial^2 \bar{u}}{\partial z^2} dz \quad \text{(Equation 31)}$$

Note the addition of 0 in Equation 31. In a typical Terzaghi's consolidation model, this term is $\bar{u}$, indicating an instantaneous application of excess pressure across the whole length of the clay. The change in unit discharge is therefore:

$$\Delta q = q_2 - q_1 = -k(i_2 - i_1) = \frac{-k}{\gamma_w} \left(\frac{\partial^2 \bar{u}}{\partial z^2} dz - \frac{\partial \bar{u}}{\partial z} \right) \quad \text{(Equation 32)}$$

The change in discharge with time is the same as the water volume loss with respect to time, which in itself is equal to the change of void volume with time (since the solid matrix is assumed to be incompressible). Nothing that the problem is one-dimensional, it's also equal to the change of vertical strain with time. This can be translated with Equation 33.

$$\Delta q = \frac{\partial \varepsilon_z}{\partial t} dz \quad \text{(Equation 33)}$$

where ε_z is the axial strain

The coefficient of compressibility m_v, defined as the ratio of in volumetric strain to change of effective stress, can be introduced at this point. It can be written in terms of the parameters of interest as follows:

$$m_v = \frac{\varepsilon_z}{\Delta\sigma'} = \frac{\varepsilon_z}{-\Delta u_e} = \frac{\varepsilon_z}{\bar{u} - \bar{u_i}} \qquad \text{(Equation 34)}$$

where ε_z is the axial strain

$\Delta\sigma$' is the change in effective stress

$\bar{u_i}$ is the initial increase in pore water pressure

Combining Equations 32, 33 and 34 yields

$$\frac{\partial[m_v(\bar{u} - \bar{u_i})]}{\partial t} dz = \frac{k}{\gamma_w}\left(\frac{\partial^2 \bar{u}}{\partial z^2} dz - \frac{\partial \bar{u}}{\partial z}\right) \qquad \text{(Equation 35)}$$

Further simplifying, the following differential equation describing the flow of water is:

$$\frac{\partial \bar{u}}{\partial t} = \frac{k}{m_v \gamma_w}\frac{\partial^2 \bar{u}}{\partial z^2} - \frac{k}{m_v \gamma_w}\frac{1}{dz}\frac{\partial \bar{u}}{\partial z} \qquad \text{(Equation 36)}$$

Equation 36, which describes the theoretical model of the change in excess pore water pressure in a pulse test, can be compared to the consolidation equation proposed by Terzaghi. The left hand side and the first term on the right-hand side is Terzaghi's differential equation, where $\frac{k}{m_v \gamma_w}$ is replaced by the coefficient of consolidation term, c_v.

Equation 36 is applied to describe the pore pressure response in the clay shown in Figure 13(a). However, to solve this equation, 2 boundary conditions are needed. The lower boundary condition is not well defined in the schematic of Figure 13(a). To solve this problem, the observation that the specimen can be mirrored about its lower boundary can be made. The model can be equivalently represented as in Figure 13(b) below.

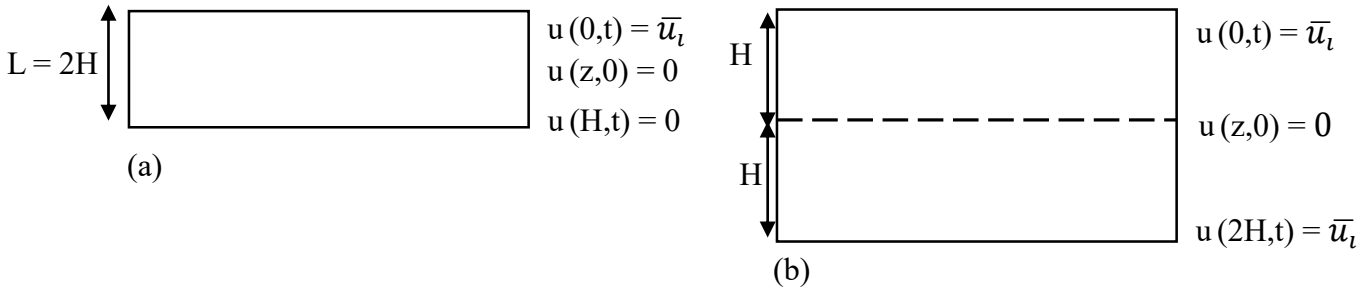

Figure 13 (a) Original soil model (b) Modified soil model

The superposition of the pore pressure diffusion of an excess pressure $\bar{u}_i$ from the top and the bottom over a length of H (as shown in Figure 13(b)) is the same as the diffusion of that same pressure increase from the top travelling a length of 2H.

The model on which the equation will be applied being the one in Figure 13(b), the term 1/dz in Equation 36 can be replaced by 1/(L/2) = 2/L.

The analytical solution to Equation 36 is:

$$\bar{u}(z,t) = \bar{u}_i + \sum_{n=0}^{\infty} c_n e^{-\frac{b}{2a}z} \sin\left(\frac{n\pi z}{L}\right) e^{\left(-\frac{an^2\pi^2}{L^2} - \frac{b^2}{4a}\right)t} \qquad \text{(Equation 37)}$$

With

$$c_n = \frac{4a\bar{u}_i\left[2\pi an + be^{\frac{bL}{2a}}\sin(\pi Ln) - 2\pi ane^{\frac{bL}{2a}}\cos(\pi Ln)\right]}{(b^2 + 4\pi^2a^2n^2)L}$$

$$a = \frac{k}{m_v\gamma_w}$$

$$b = -\frac{k}{m_v\gamma_w}\frac{1}{dz}$$

The derivation of the solution can be found in the Appendix. This derived equation will be compared with laboratory data to verify its validity. It will also help determine the diffusivity factor that controls the pore pressure response due to pressure pulses at the top. Since this factor has the same definition as the coefficient of consolidation derived in Terzaghi's theory, it will be referred

to by the same notation, c_v. To differentiate between this factor and Terzaghi's c_v, it will be necessary at some points in this paper to add the suffix "pulse" or "cons".

One of the main applications of this model is the prediction and the description of the groundwater response in a body subjected to a change in pore pressure (such as rainfall, excess pore pressure at a shearing plane,…).

4 EXPERIMENTAL PROCEDURES

The experimental procedures listed in this chapter includes those of the new consolidation tests performed in this study along with those from Brewster (2015) for the pulse tests. The pulse tests analyzed in the following Chapter were reported by Brewster (2015) and the new proposed model was applied to these data in this thesis.

4.1 Introduction

The purpose of the experimental program is to examine the factors that affect the pore pressure diffusion process in a high plasticity clay. It is divided into 3 major areas of focus:

1. Test out the pore pressure diffusion model presented in Section 3 on saturated and consolidated samples of clay. To perform this comparison, a series of "pulse" tests are run after primary consolidation for different consolidation pressures.
2. Observe the difference between coefficients of diffusion controlling typical consolidation tests (where change in total stress is experienced at every point in a clay specimen) and pulse tests. Based on the model that has been presented in Section 3, the diffusion coefficient that is to be found in a pulse test has the same definition as Terzaghi's coefficient of consolidation in a typical consolidation test. This analysis will help determine the reasons behind the discrepancies between that same defined parameter in the two different types of testing.
3. Measure the pore water pressure response of a sample of clay under consolidation due to simultaneous effects of diffusion and one-dimensional consolidation in a CRS setup.

The procedure for each of these points is described below.

4.2 Brewster (2015) Specimen Preparation and Testing

Pore pressure pulse tests were conducted by Brewster (2015). The following description is a list of experimental details that are summarized to simplify the reader's access to the information.

4.2.1 Preparation of the clay specimen

The clay in use in these experiments is fire clay of a moisture content of 50%, molded into a cylinder with a diameter of 2.5 in. The moisture content is chosen such that the clay specimen becomes plastic enough to retain its shape during the process of molding and transfer to a

consolidation cell. The cell is equipped with a top and bottom drainage line and a loading frame with a load cell. The clay sample is placed between 2 filter papers and 2 porous stones. The filter papers are and the porous stones are soaked beforehand, and the bottom of the consolidation cell is flushed to ensure saturation.

Initial calculations are made to the specimen's initial bulk and void ratio.

4.2.2 Back pressure saturation

Back pressure saturation is performed by increasing cell and back pressure by increments of 10 kPa, with the top and bottom drainage line open. After every increase, inflow and outflow valves of the consolidation cell are closed to perform a B-value check. A B-value of 0.95 is an acceptable value to confirm that the clay specimen is saturated.

4.2.3 Hydraulic conductivity

Hydraulic conductivity tests using the falling head, rising tail procedure outlined in ASTM 5084 were performed.

4.2.4 Consolidation

A pressure increment is applied on the clay specimen while both the inflow and outflow valves are closed. Afterward, the inflow valve is opened. With the specimen constrained at its sides, this creates a one-dimensional, one-way drainage consolidation environment, where water is expelled from the top. Readings of pressure are recorded at the bottom of the clay sample with a pore pressure transducer (that has also been flushed), and LVDT measurements monitor the change in height with time.

4.2.5 Pulse test setup

After saturating the specimen, a pulse test is performed on it. This test consists of applying an increment of pressure in the inflow burette of the clay sample, while both inflow and outflow valves are closed. Then, the inflow valve is opened and pressure equalization is measured at the bottom of the sample. A plot of pressure vs time can be obtained at the lower boundary.

Increments of pressure used for consolidation and pulse tests were 100 kPa, 150 kPa and 200 kPa. Two sets of experiments are performed on the same clay. They will be referred to as FC-CRS1 and FC-CRS2.

4.3 Modified CRS Consolidation tests

For point 3 in the experimental objectives, a fire clay specimen has been reconstituted under a 20 psi vertical stress. The specimen is then removed and placed in a CRS setup under a vertical stress of 2 psi. The cell is equipped with top and bottom drainage lines, one pressure transducer and is loaded using a GeoJack loading frame with a load cell and an LVDT. The specimen is backpressure saturated using the flow pump with both top and bottom drainage lines open. The vertical stress was then increased to 10 psi, 20 psi, 30 psi and 40 psi and the specimen was allowed to consolidate at each of these stress levels while the pore pressures at the base and the vertical surface displacements were recorded. The initial water content of the clay is calculated to be 34.21%.

5 RESULTS AND ANALYSIS

5.1 Introduction

This chapter presents the experimental data collected with the pulse tests and the modified CRS consolidation tests in tabular form and graphical methods. It also compares the numerical pulse model with the laboratory data, compares the factors that control pore pressure propagation in each case.

A comprehensive set of data is presented below. The variables used in these tables is listed as follows:

k	Hydraulic conductivity
K	Permeability
c_v (cons)	Coefficient of consolidation
c_v (pulse)	Pulse diffusion coefficient
t_{EOP}	Time at end of primary consolidation
ε	Strain
σ’	Effective stress
e_0	Initial void ratio
H_0	Initial height of specimen
φ	Porosity
β	Compressibility coefficient

Table 1 Results from consolidation and pulse tests for the FC-CRS1 data set

100 kPa consolidation		
k	2.95×10^{-9}	cm/s
c_v (cons)	3.36×10^{-5}	cm^2/s
t_{EOP}	19600	s
Strain at EOP	1.05%	
dε/dσ' (experimentally)	2.10×10^{-4}	KPa^{-1}

100 kPa pulse		
k	2.95×10^{-9}	cm/s
c_v (pulse)	2.30×10^{-4}	cm^2/s
dε/dσ'	1.31×10^{-4}	KPa^{-1}
Δσ'	2	kPa
dε	0.03%	

150 kPa consolidation		
k	2.95×10^{-9}	cm/s
c_v (cons)	2.27×10^{-5}	cm^2/s
t_{EOP}	4096	s
Strain at EOP	0.41%	
dε/dσ' (experimentally)	8.20×10^{-5}	KPa^{-1}

150 kPa pulse		
k	2.95×10^{-9}	cm/s
c_v (pulse)	2.31×10^{-4}	cm^2/s
dε/dσ'	1.30×10^{-4}	KPa^{-1}
Δσ'	2	kPa
dε	0.03%	

200 kPa consolidation		
k	2.55×10^{-9}	cm/s
c_v (cons)	2.05×10^{-5}	cm^2/s
t_{EOP}	6084	s
Strain at EOP	0.36%	
dε/dσ'	7.28×10^{-5}	KPa^{-1}

200 kPa pulse		
k	2.55×10^{-9}	cm/s
c_v (pulse)	2.30×10^{-4}	cm^2/s
dε/dσ'	1.13×10^{-4}	KPa^{-1}
Δσ'	2	kPa
dε	0.02%	

Table 2 Results from consolidation and pulse tests for the FC-CRS2 data set

100 kPa consolidation		
k	3.09×10^{-9}	cm/s
c_v (cons)	4.45×10^{-5}	cm^2/s
t_{EOP}	3600	s
Strain at EOP	0.63%	
dε/dσ' (experimentally)	1.27×10^{-4}	

100 kPa pulse		
k	3.09×10^{-9}	cm/s
c_v (pulse)	1.00×10^{-4}	cm^2/s
dε/dσ'	3.15×10^{-4}	KPa^{-1}
Δσ'	2.2	kPa
dε	0.07%	

150 kPa consolidation		
k	2.9×10^{-9}	cm/s
c_v (cons)	4.02×10^{-5}	cm^2/s
t_{EOP}	3364	s
Strain at EOP	0.43%	
dε/dσ' (experimentally)	8.57×10^{-5}	

150 kPa pulse		
k	2.90×10^{-9}	cm/s
c_v (pulse)	1.17×10^{-4}	cm^2/s
dε/dσ'	2.53×10^{-4}	KPa^{-1}
Δσ'	2.2	kPa
dε	0.06%	

200 kPa consolidation		
k	2.34×10^{-9}	cm/s
c_v (cons)	6.35×10^{-5}	cm^2/s
t_{EOP}	14400	s
Strain at EOP	0.42%	
dε/dσ' (experimentally)	8.45×10^{-5}	

200 kPa pulse		
k	2.34×10^{-9}	cm/s
c_v (pulse)	1.74×10^{-4}	cm^2/s
dε/dσ'	1.37×10^{-9}	KPa^{-1}
Δσ'	2.2	kPa
dε	0.03%	

Table 3 Parameters and results for the CRS tests

Consolidation pressure (psi)	**10**	**30**	**40**
e_0	0.866	0.772	0.695
H_0 (in)	0.865	0.821	0.786
c_v (in/sec)	4.50×10^{-5}	1.27×10^{-5}	1.41×10^{-5}
k (cm/sec)	4.54×10^{-9}	4.50×10^{-9}	3.70×10^{-9}
K (in^2)	6.39×10^{-15}	6.33×10^{-15}	5.21×10^{-15}
φ	0.464	0.435	0.410
β (psi^{-1})	3.69×10^{-6}	3.00×10^{-6}	4.78×10^{-6}

5.2 c_v results from consolidation tests

Coefficient of consolidation results for the consolidation tests are obtained graphically from the displacement vs. time graph. The square root of time method was adopted for that purpose. This method is an indicator of the time at which 90% consolidation occurs. The end of primary consolidation can be deduced accordingly. Figure 14 is the displacement vs time plot for the sample of clay under 150 kPa consolidation pressure in the FC-CRS1 set of test. It is an illustration of the first step taken in this method. The two red lines are the first tangent, and that tangent shifted by a multiplication factor of 1.15, respectively. The intersection of those lines with the y-axis is taken as the displacement at time 0. Note that the first tangential is hard to pinpoint in this graph (which was also the case for almost all similar consolidation graphs for different confining pressures). The first few 1/1000ths of an inch of displacement are considered to be immediate settlement under the applied increment of pressure. Values of c_v(cons) for each set of experiments (FC-CRS1 and FC-CRS2) are recorded in Table 1 and Table 2

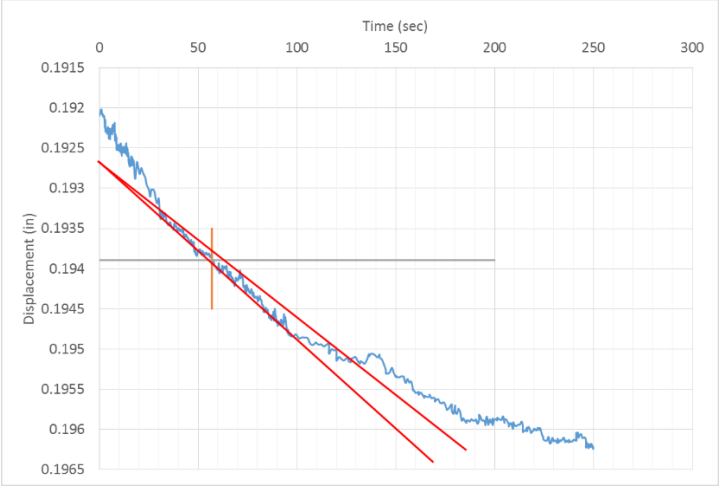

Figure 14 Square root of method to identify c_v for the FC-CRS1 clay sample under 150 kPa consolidation pressure

5.3 c_v results of pulse tests

The theoretical model for pore pressure diffusion presented by Equation 37 (Section 3.2) was applied to the pulse tests performed on the clay sample in the modified CRS setup. The calculations were first run with a value for c_v obtained from consolidation tests. Then, the RMS error between the experimental pore water pressures vs time recorded at the bottom of the clay and the analytical values was calculated for that particular value of c_v. This value was then optimized using the "Solver" function in Microsoft Excel to its minimum. This minimum provided a set of theoretical values that best matched the laboratory data.

Figure 15 to Figure 17 show the graphical results of the pore pressure measurements for the pressure increments of 100, 150 and 200 kPa in the CRS setup. In blue is the analytical curve using the optimized value of c_v(pulse). The analytical model provides a very good fit to the experimental data. The optimized c_v(pulse) results for each pressure pulse increase and for each set of experiments (FC-CRS1 and FC-CRS2) are recorded in Table 1 and Table 2.

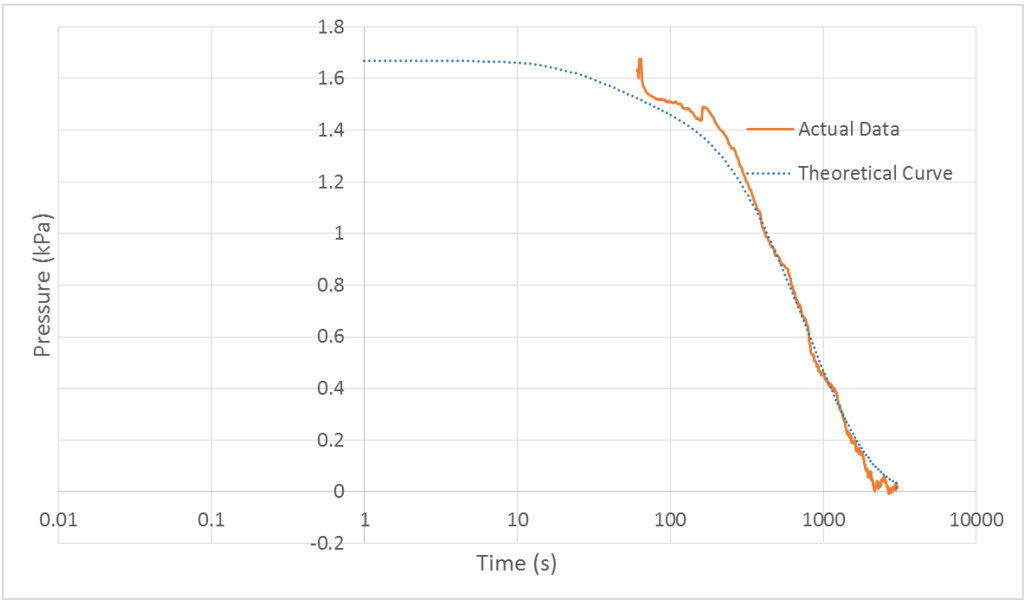

Figure 15 FC-CRS1 100 kPa

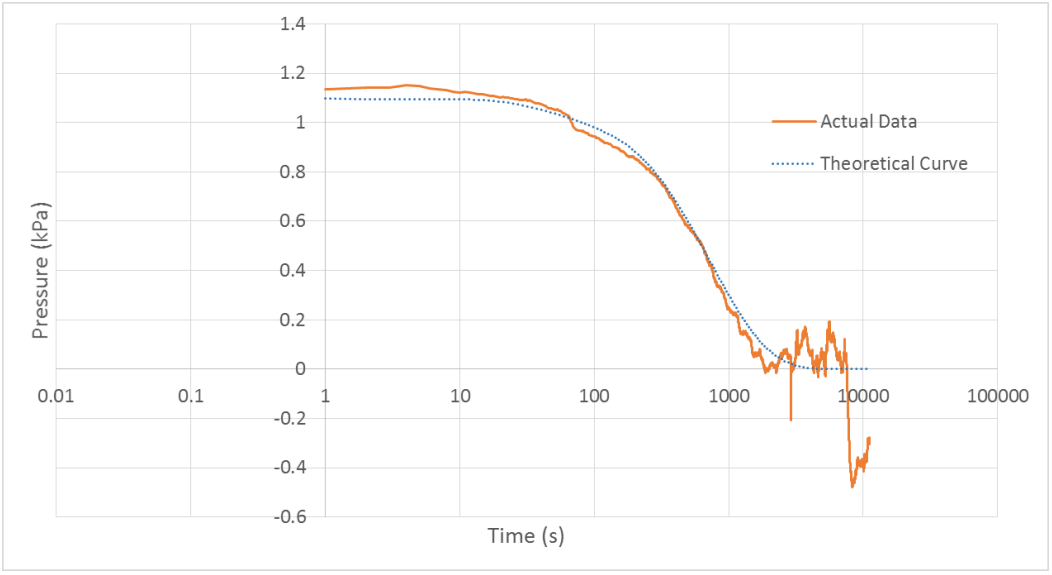

Figure 16 FC-CRS1 150 kPa

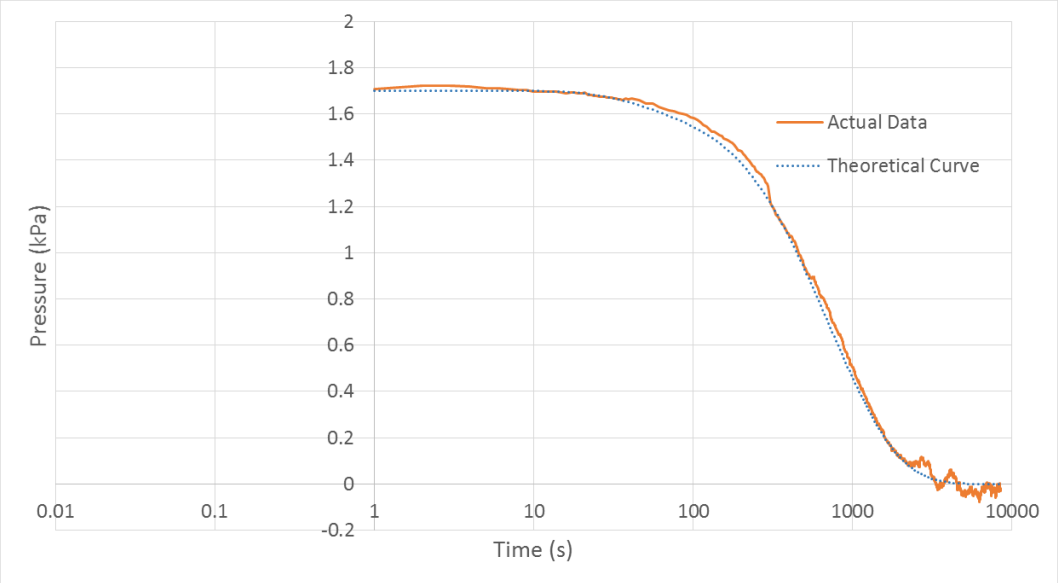

Figure 17 FC-CRS1 200 kPa

5.4 Comparison between c_v (pulse) and c_v (cons)

The c_v values obtained by conducting pulse tests are compared with the c_v obtained with conventional consolidation tests. The parameter c_v is defined the same way in both cases, being equal to:

$$c_v = \frac{k}{m_v \gamma_w}$$

The values of c_v obtained using both tests are expected to be different because of the different boundary conditions in each of the procedures, which result in different gradients across a sample of clay. The comparison will help identify the factors that affect how pore pressure propagates in each case.

Due to the difference in the nature of the applied pressure in each type of situation, it may be beneficial to look at how the direction of the pressure change creates a different pattern of pressure response. In typical consolidation tests, pressure decreases with time. In pulse tests, the opposite happens: the diffusion waves reaching a specific depth in a clay body increase the pressure at the depth (followed by an eventual decrease due to drainage). This difference in pressure change must be accompanied by different stiffnesses in each kind of test.

To investigate the effect of this difference on the value of c_v, it is helpful to look at processes that are equivalent when it comes to the direction of pressure change. Since pressure increases with time in pulse tests, the equivalent process would be an unloading sequence of consolidation. Therefore, looking at stiffness differences in loading vs unloading consolidation situations may help explain the difference between c_v(cons) and c_v(pulse).

The author was able to access loading and unloading incremental consolidation tests, performed on a fire clay sample with an initial void ration of 0.873. The confining pressure is 4000 psf (about 200 kPa). The ratio of strain between loading and unloading will be compared to the ratio of c_v(cons) ad c_v(pulse).

Stiffness in a consolidation test is defined as $d\varepsilon/d\sigma'$, $d\varepsilon$ being the change in strain at the end of primary consolidation and $d\sigma'$ being the increment of pressure that is added before consolidation happens. $d\varepsilon$ can be obtained graphically by looking at the log of time vs displacement graph and detecting the displacement at which the slope of the curve shifts slopes.

For the incremental loading test at 4000 psf, $d\varepsilon/d\sigma' = 8.67\times10^{-4}\ KPa^{-1}$.

For the incremental unloading test at 4000 psf, $d\varepsilon/d\sigma' = 2.18\times10^{-3}\ KPa^{-1}$.

Thus, $(d\varepsilon/d\sigma')_{unloading} / (d\varepsilon/d\sigma')_{loading} = 2.5$.

This value can be compared to c_v(pulse)/c_v(cons) obtained at 200 KPa (which is about 4000 psf). That value is about 11 for the FC-CRS1 data and 2.74 for the FC-CRS2 data (refer to summary Table 1 and Table 2). Other ratios from similar tests in the past (Brewster, 2015) have resulted in ratios of c_v's ranging anywhere from 0.2 to 2 orders of magnitude.

Obviously, the available data for comparison is very limited, and while these ratios are not conclusive in any way, it shows that the effect of "unloading" in a pulse test affects the propagation of water in the clay.

5.5 Comparison between pulse equation and Terzaghi's consolidation equation

An interesting comparison to perform is the effect that the different mechanisms caused by the pulse model and a typical consolidation model have on the variation of pressure over time in a

clay. The comparison can be made by studying how different the results of the equations representing these two processes are when taking the same coefficient of diffusion in each case. This is illustrated in Figure 18, where three curves are superimposed:

- The curve called "Actual data" is the experimental plot of pore pressure at the bottom of a clay specimen vs time during a pulse test
- The curve called "Analytical diffusion for pore pressure propagation" represents the analytical solution to the pulse equation derived in Section 3. This curve was obtained using a coefficient of diffusion c_v(pulse).
- The curve called "Terzaghi's consolidation equation" represents the analytical solution to Terzaghi's model, while using the same c_v(pulse).

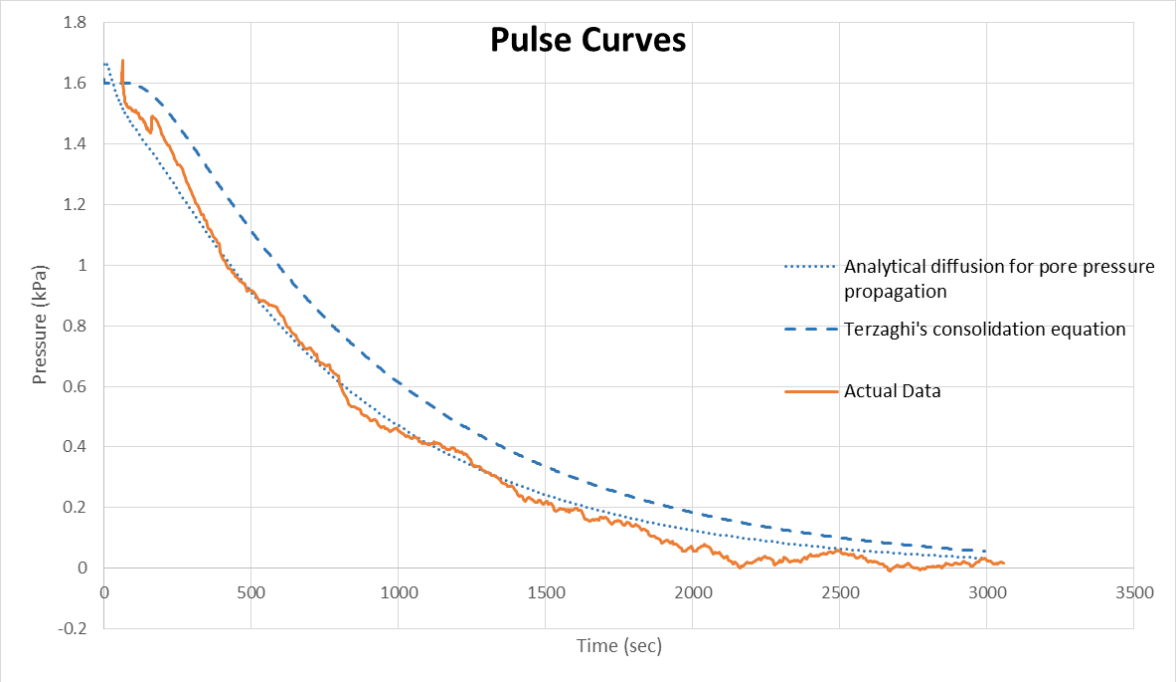

Figure 18 Comparison between pulse curve and Terzaghi's consolidation curve

Both analytical curves use the same coefficient c_v. What can be concluded from this comparison is that applying the pulse model shifts Terzaghi's consolidation results with time.

This difference can be observed by comparing the differential equations of both models. Terzaghi's differential equation of consolidation is:

$$\frac{\partial \bar{u}}{\partial t} = \frac{k}{m_v \gamma_w} \frac{\partial^2 \bar{u}}{\partial z^2}$$

The pulse model for pore pressure diffusion, on the other hand, has the differential equation derived earlier in Section 3:

$$\frac{\partial \bar{u}}{\partial t} = \frac{k}{m_v \gamma_w} \frac{\partial^2 \bar{u}}{\partial z^2} - \frac{k}{m_v \gamma_w} \frac{1}{dz} \frac{\partial \bar{u}}{\partial z}$$

The term $-\frac{k}{m_v \gamma_w} \frac{1}{dz} \frac{\partial \bar{u}}{\partial z}$ in the pulse model is the one that is responsible for the shifting observed in the graph above. This term makes the slope of the line more negative, which means that the pressure is diffusing faster with time.

6 MODELING PORE PRESSURE DIFFUSION AND CONSOLIDATION SIMULTANEOUSLY

Looking at pore pressure diffusion and consolidation processes, the best way to describe their interaction together is to analyze them acting simultaneously on a clay specimen. For that purpose, a CRS test was conducted on a specimen of fire clay to monitor its consolidation process. The two interconnected processes are taking place in the clay sample and they affect the pore water pressure recorded at the bottom as follows.

6.1 Pore pressure diffusion

The first process is pore pressure diffusion. When an incremental load is applied, an incremental stress (load divided by area of contact) is exerted on top of the specimen. Together with the initial stress before the time of application, this constitutes the stress at time 0. Due to the time lag effect of the pore pressure diffusion discussed in Section 2.2.2, it will take time for the applied pressure to be felt at the bottom of the specimen. The pressure diffusion-induced strain is function of how compressible the solid skeleton and the water filling the voids are (Berti & Simoni, Field evidence of pore pressure diffusion in clayey soils prone to landsliding, 2009).

The diffusion coefficient D is calculated by applying Equation 14, relating it to the permeability K, the porosity φ, the compressibility β and the viscosity of the water μ. The following steps state how each of these parameters is obtained for each stage of the experimental procedure:

- The viscosity of the water is taken to be $\mu = 1.29 \times 10^{-7}$ psi.sec
- To calculate the porosity φ, the following steps were taken:
    - The initial void ratio, e_0, at the beginning of the test, is calculated using the phase relation

$$Gw_0 = Se_0 \qquad \text{(Equation 38)}$$

Where G is the specific gravity of the soil, taken to be 2.72

w_0 is the initial water content, obtained to be 34.21%

S is the degree of saturation, assumed to be 1.

The initial void ratio is therefore $e_0 = 0.93$

- The vertical deformation due to the change in applied pressure of each loading sequence, ΔH_i, is obtained from the experimental data. For purposes of this calculation, we will also calculate $\Delta H_{cum,i}$, which is the cumulative change in height at the beginning of a loading sequence, due to all past vertical stress increases:

$$\Delta H_{cum,i} = \sum_i \Delta H_i \qquad \text{(Equation 39)}$$

  Where i is the each past loading sequence

- $\Delta H_{cum,i}$ is related to $\Delta e_{cum,i}$, which is the cumulative change in void ration at the beginning of a loading sequence via the relationship between vertical deformation and void ratio:

$$\Delta e_{cum,i} = \frac{\Delta H_{cum,i}}{H_0}(1 + e_0) \qquad \text{(Equation 40)}$$

- The void ratio at the beginning of each loading sequence, e_{ini}, is then deduced from e_0 and $\Delta e_{cum,i}$.

$$e_{ini} = e_0 - \Delta e_{cum,i} \qquad \text{(Equation 41)}$$

- Finally, the porosity φ is obtained using this relationship:

$$e_{ini}\varphi = \frac{e_{ini}}{1 + e_{ini}} = e_0 - \Delta e_{cum,i} \qquad \text{(Equation 42)}$$

- The hydraulic conductivity k was not measured experimentally, so it was back-calculated using the definition of the coefficient of consolidation:

$$c_v = \frac{k\Delta\sigma}{\epsilon\gamma_w} \Leftrightarrow k = \frac{c_v\epsilon\gamma_w}{\Delta\sigma} \qquad \text{(Equation 43)}$$

  Where c_v is the coefficient of consolidation

  Δσ is the increase in vertical stress

  ε is the change in strain at the end of primary consolidation

- The compressibility β is a property of the material that is being tested. By referring to Biot's theory of poroelasticity (refer to Section 2.1.4), it is related to the bulk modulus of

the pore system and the solid particles. Due to lack of numerical values, the best that can be done is to approximate β from values of bulk moduli in the literature, which was not opted here. Instead, β will be optimized at the end of the analysis process, so that the theoretical model fits the experimental data.

The values of ΔH, Δe, φ, c_v, ε and optimized values of β are shown in Table 3.

The pore pressure propagation will be modeled using Equation 17, which for convenience is repeated below:

$$u = \bar{u}\left[1 - \text{erf}\left(\frac{z}{2\sqrt{Dt}}\right)\right]$$

Since measuring the pore pressure at the bottom of the specimen is of interest, assign z = H.

6.2 Consolidation

The second process is consolidation. An increase in total stress causes an increase in pore water pressure in a low permeability soil. Over time, the load carried by the water is transferred to the solid particles. Water is expelled and the effective stress of the soil increases. The rate of water drainage out of the soil dictates the rate of settlement.

The coefficient of consolidation c_v is found for every incremental pressure using the log of time method. Figure 19 shows an example of the procedure needed to get c_v for the clay specimen subjected to the vertical stress of 30 psi.

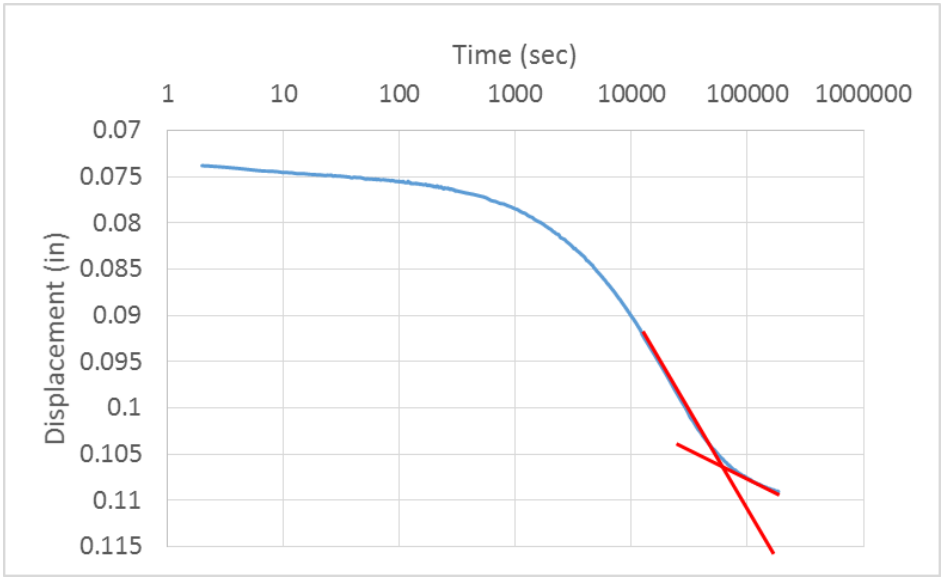

t_2	500	sec
s_2	0.0771	in
t_1	125	sec
s_1	0.0756	in
Δs	0.0015	in
s_0	0.0741	in
s_{100}	0.1066	in
s_{50}	0.09035	in
t_{50}	10000	sec
c_v	1.33×10^{-5}	in^2/sec

Figure 19 Log of time method for the clay specimen under 30 psi vertical stress

The values of c_v for all CRS tests are compiled in Table 3.

6.3 Modeling the pore pressure

The pore pressure diffusion and the consolidation happen simultaneously. As soon as pressure diffuses to a certain depth in the soil, this pressure begins to decrease due to the expulsion of the water. Terzaghi's consolidation theory considers that the increase in total stress $\Delta\sigma$ (and therefore the increase in pore water pressure $\bar{u}$) occurs instantaneously and uniformly across the soil. However, this does not consider the fact that the pressure difference has to diffuse from the top to the bottom first. Therefore, the pressure difference experienced at the bottom (and at any depth for that matter) increases from 0 to $\bar{u}$ over a certain period of time after the load application.

A way to visualize the interaction of these two processes together is by changing the term $\bar{u}$, which refers to applied pressure at the top, in Equation 17 to $\bar{u}$(t). $\bar{u}$(t) is defined as follows:

$$\bar{u}(t) = \bar{u_i} \times [1 - U(t)] \qquad \text{(Equation 44)}$$

where U is the degree of consolidation described in Equation 24.

Equation 17 therefore becomes

$$u = \bar{u}(t) \times \left[1 - \text{erf}\left(\frac{H}{2\sqrt{Dt}}\right)\right] \qquad \text{(Equation 45)}$$

What the above equation indicates is that the pressure difference $\bar{u_i}$, applied at the top of the specimen, is diffused to the depth H at time t, but this pressure difference is itself dissipating with time due to consolidation.

In Equation 38, $\bar{u_i}$ is theoretically equal to the increase in total stress (the increase of pore pressure at the top). Realistically, in the laboratory setting, it takes a few seconds for the incremental stress to apply. To increase accuracy of the analysis, instead of taking a constant $\bar{u}$ at every point in time, the difference in applied stress $\Delta\bar{u}$ will be adopted, as indicated in Equation 46.

$$\Delta\bar{u}(t) = \bar{u}_t - \bar{u}_0 \qquad \text{(Equation 46)}$$

where $\bar{u}_t$ and $\bar{u}_0$ are the increments of pressures at time t and 0, respectively.

$\Delta\bar{u}$ increases from 0 to $\bar{u}_i$ in a matter of seconds.

Combining Equations 17, 44, 45 and 46, Equation 47 below is what describes the change in pore water pressure in the clay specimen:

$$u(t) = (\bar{u}_t - \bar{u}_0)\left[1 - \left[\frac{\left(\frac{c_v t}{H^2}\right)^3}{\left(\frac{c_v t}{H^2}\right)^3 + 0.5}\right]^{1/6}\right] \times \left[1 - \text{erf}\left(\frac{H}{2\sqrt{Dt}}\right)\right] \quad \text{(Equation 47)}$$

An additional observation to make is the fact that the distance traveled by the front of the propagation wave is not always H; it rather decreases with decreasing time. It starts from H and then decreases at a rate equal to the rate of decrease in the degree of consolidation.

Figure 20 to Figure 22 display the experimental pore water pressure at the bottom of the clay vs the analytical solution to the diffusion problem, for the three different consolidation pressures: 10, 30 and 40 psi.

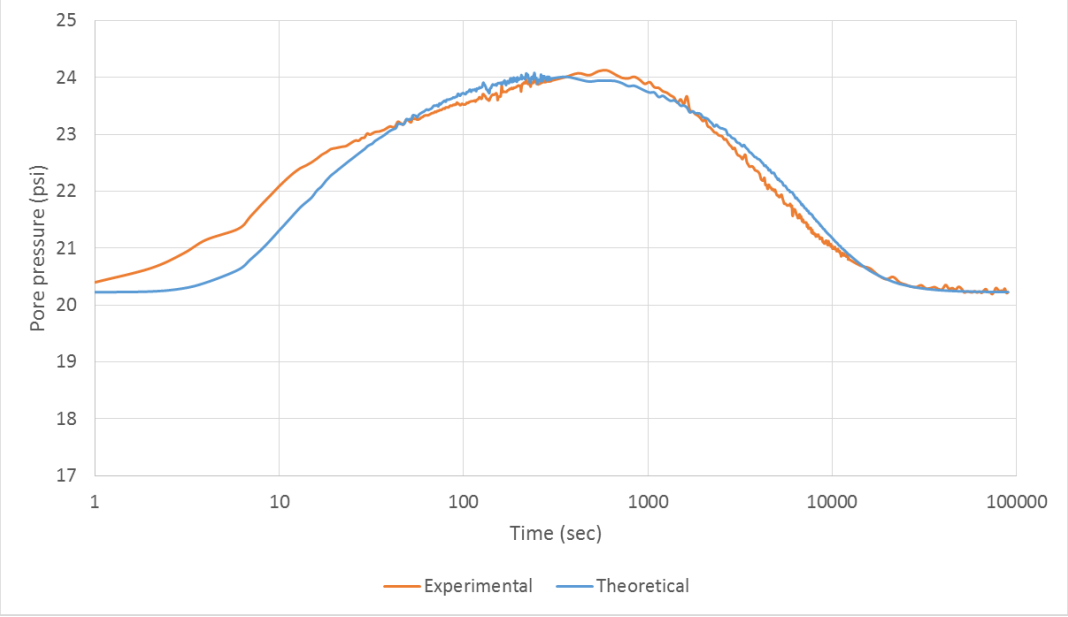

Figure 20 Experimental pore pressure results and analytical solutions for the specimen under a vertical stress of 10 psi

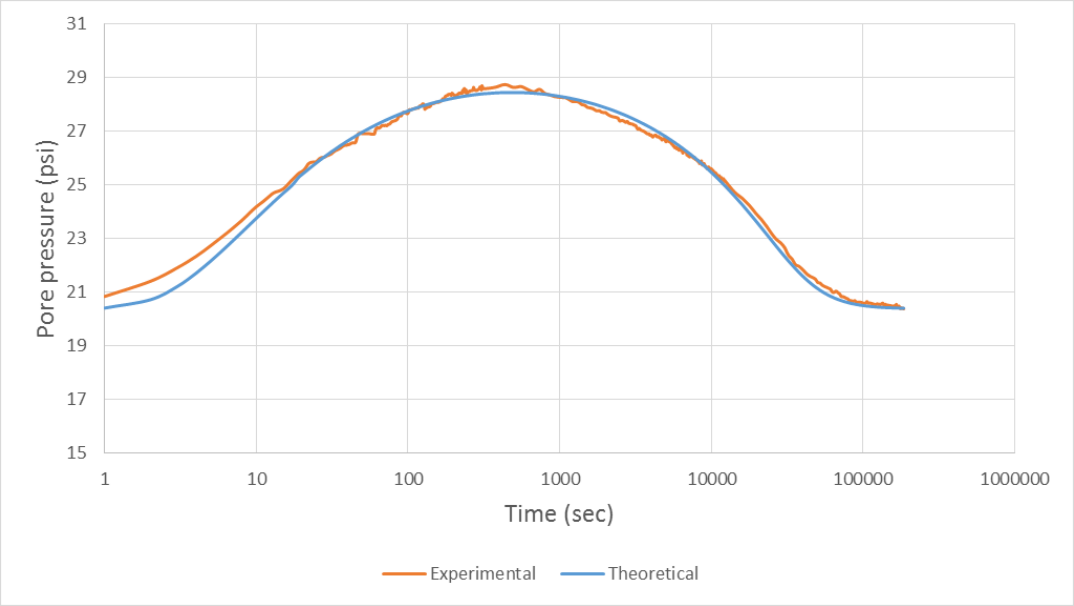

Figure 21 Experimental pore pressure results and analytical solutions for the specimen under a vertical stress of 30 psi

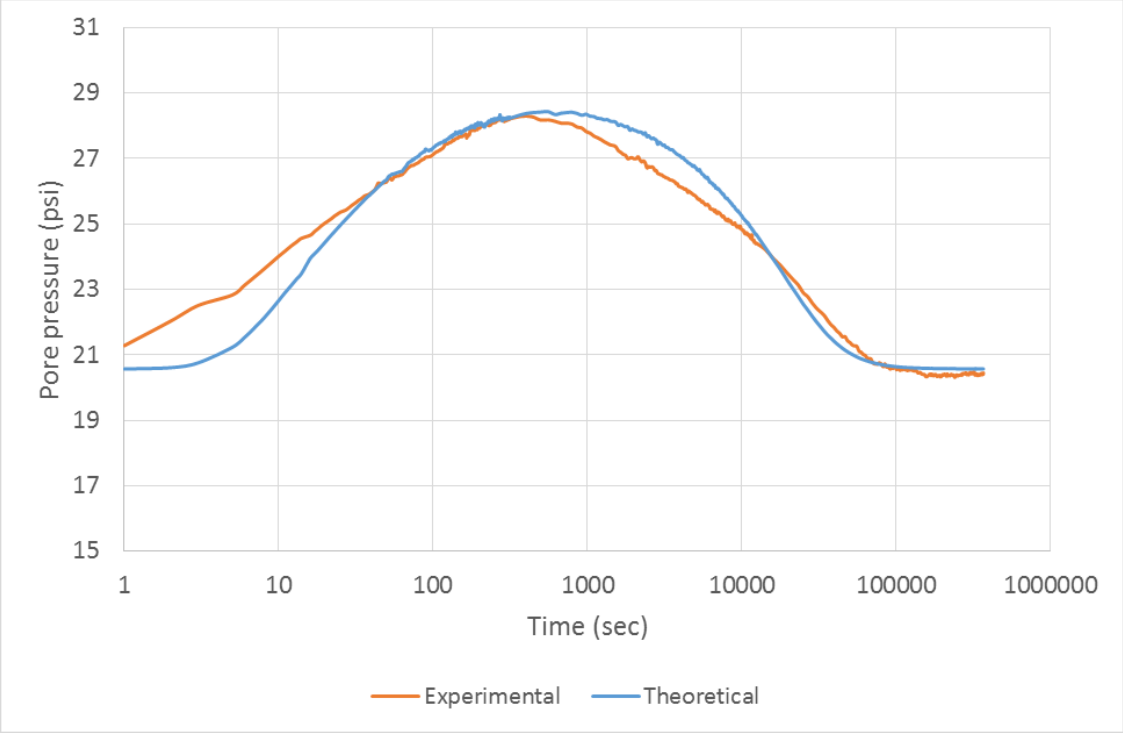

Figure 22 Experimental pore pressure results and analytical solutions for the specimen under a vertical stress of 40 psi

6.4 Finite difference analysis

A more precise approach to tackle the problem is numerically, using a finite difference methodology. The reason behind this choice is to make sure that the problem is not oversimplified

by the assumptions that are considered, which may lead to less accuracy. Solving the problem numerically, although needing more computational effort, leads to increased accuracy.

6.4.1 Reinstating the problem

For the sake of this particular section, the differential equation under study will be repeated:

$$\frac{\partial u}{\partial t} = D\frac{\partial^2 u}{\partial z^2} \qquad \text{(Equation 48)}$$

- Boundary conditions:

  $u(0,t) = \bar{u_\iota}\left(1 - \left[\frac{(T_v)^3}{(T_v)^3 + 0.5}\right]^{1/6}\right)$

  $u(\infty, t) = 0$

- Initial condition:

  $u(z,0) = 0$

Finite differences are discretization methods that deal with approximating differential equations with difference equations over smaller increments. These equations are derived from Taylor's polynomial approximations, and therefore can increase in accuracy if the degree of the truncation error increases. The choice of finite differences can be between forward, backward and central differences. The selection of any of these (or a combination of them) depends of the accuracy needed to solve the problem, as well as the need of obtaining a stable solution to the differential equation. There are two approaches to using finite difference:

- The explicit method: by using this method, all the unknowns at all the nodes can be calculated at time t+1 by knowing the values of those same unknowns at time t.
- The implicit method: at each time increment t, the needs arises to solve a system of equations to simultaneously solve for the unknowns at the different nodes at a specific time t.

A particular advantage of using the implicit method over the explicit method is that the explicit method can sometimes result in unstable solutions, a problem that is not found in the implicit one. Another benefit with the implicit method is that the time increments Δt do not have to be equal. These advantages are at the expense of a greater computational effort, but ensure a better accuracy.

The specimen is divided into 10 elements of equal length, giving a total of N = 11 nodes. The length of each node is H/10 = 0.82 in / 10 = 0.082 in. The first node is at the upper boundary. Each

subsequent node will be the numerical measure of the pore water pressure at the bottom of each element. To obtain an even better approximation, the time increments have also been reduced from 1 sec to 0.1 sec.

The first step is to set the initial condition: every node is the system has an initial pressure of 0. Then the upper and boundary conditions are assigned. The upper boundary condition changes with time as a function of T_v. The lower boundary condition in the differential equation is indicated as infinity. What the lower boundary condition basically means is that at great depths, the pore pressure increase would not be felt. Since an actual boundary condition is needed to numerically solve the problem, this problem can be fixed by creating imaginary nodes that tend to approach a reasonable infinity depth, relative to the problem at hand. For this reason, instead of opting for 11 nodes (10 elements) only, the number of these nodes can be increased to a big number. N is chosen to be 100, and the incremental depth is still equal to 0.082 in. This initial procedure is shown in the schematic of Figure 23.

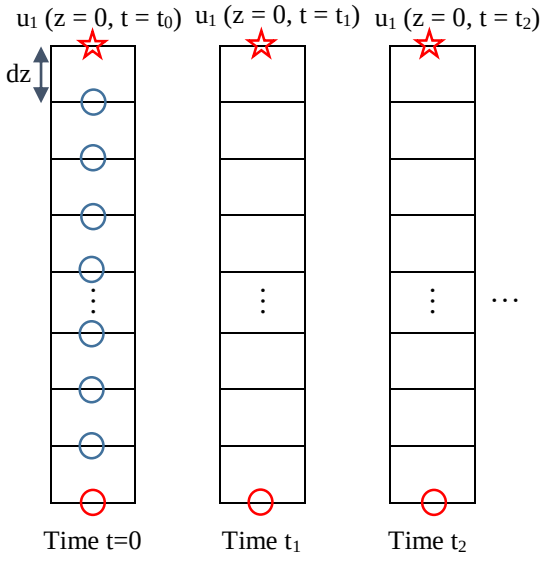

Figure 23 Numerical formulation of the pore pressure diffusion problem

6.4.2 Crank-Nicolson method

The Crank-Nicholson method is chosen as an implicit method to solve the differential equation. The forward difference approximation is used for $\partial u/\partial t$, to estimate the approximate average value for the time period t_i to t_{i+1}.

$$\frac{\partial u}{\partial t} = \frac{u_{i,t+1} - u_{i,t}}{\Delta t} \qquad \text{(Equation 49)}$$

$\partial^2 u/\partial z^2$ should also be approximated as the average of t_i to t_{i+1}. For that purpose, the central difference is taken at these two times and averaged.

$$\frac{\partial^2 u}{\partial z^2} = \frac{1}{2}\left[\frac{u_{i-1,t} - 2u_{i,t} + u_{i+1,t}}{(\Delta z)^2} + \frac{u_{i-1,t+1} - 2u_{i,t+1} + u_{i+1,t+1}}{(\Delta z)^2}\right] \qquad \text{(Equation 50)}$$

Substituting Equations 49 and 50 into Equation 48, and taking

$$\alpha = \frac{D\Delta t}{(\Delta z)^2} \qquad \text{(Equation 51)}$$

The implicit formulation of the equation becomes

$$-u_{i-1,t+1} + \frac{2(1+\alpha)}{\alpha} u_{i,t+1} - u_{i+1,t+1} = u_{i-1,t} + \frac{2(1-\alpha)}{\alpha} u_{i,t} + u_{i+1,t} \qquad \text{(Equation 52)}$$

A system of equations of 99 equations with 98 unknowns (u_2 to u_{99}) is solved at every time increment t+1 based on the values of u at time t. Each system can be written in the form of a matrix Au=b. This matrix is shown below, with the following terms used for compactness

$\beta = \frac{2(1+\alpha)}{\alpha}$ and $\beta' = \frac{2(1-\alpha)}{\alpha}$ for compactness

$$\begin{bmatrix} \beta & -1 & & & & & \\ -1 & \beta & -1 & & & & \\ & -1 & \beta & & & & \\ & & & \ddots & & & \\ & & & -1 & \beta & -1 & \\ & & & & -1 & \beta & \end{bmatrix} \begin{bmatrix} u_{2,t} \\ \vdots \\ \\ \\ \\ u_{99,t} \end{bmatrix} = \begin{bmatrix} u_{1,t-1} + u_{1,t} + \beta' u_{2,t-1} + u_{3,t-1} \\ u_{2,t-1} + \beta' u_{2,t-1} + u_{3,t-1} \\ \vdots \\ \\ u_{97,t-1} + \beta' u_{98,t-1} + u_{99,t-1} \\ u_{98,t-1} + \beta' u_{99,t-1} \end{bmatrix}$$

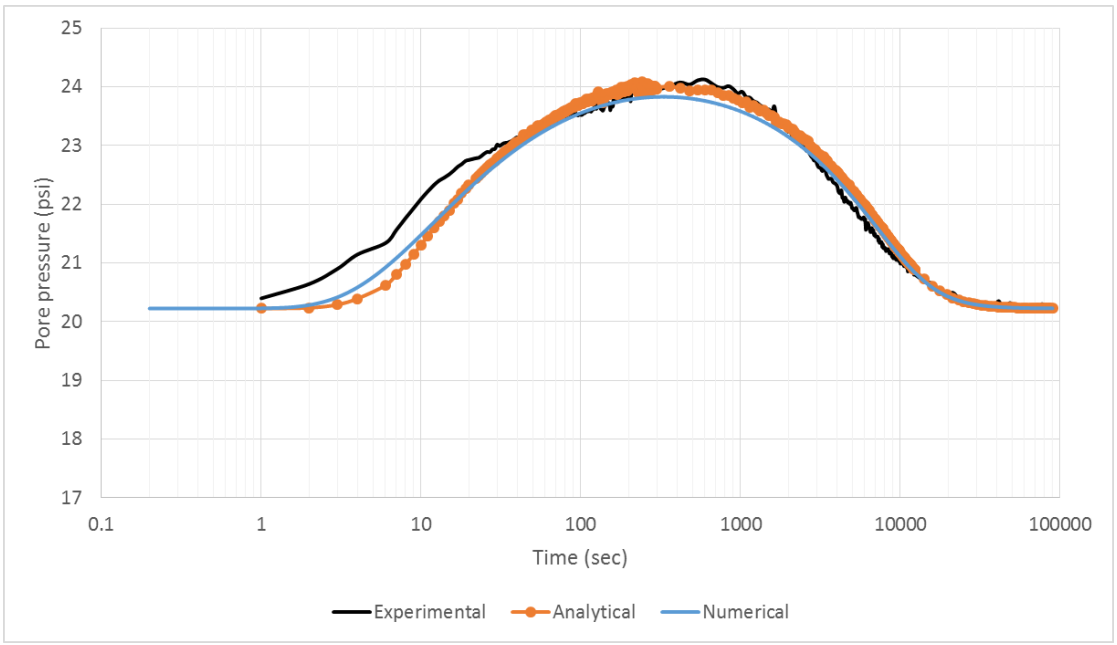

Figure 24 Experimental pore pressure results, analytical and numerical solutions for the specimen under a vertical stress of 10 psi

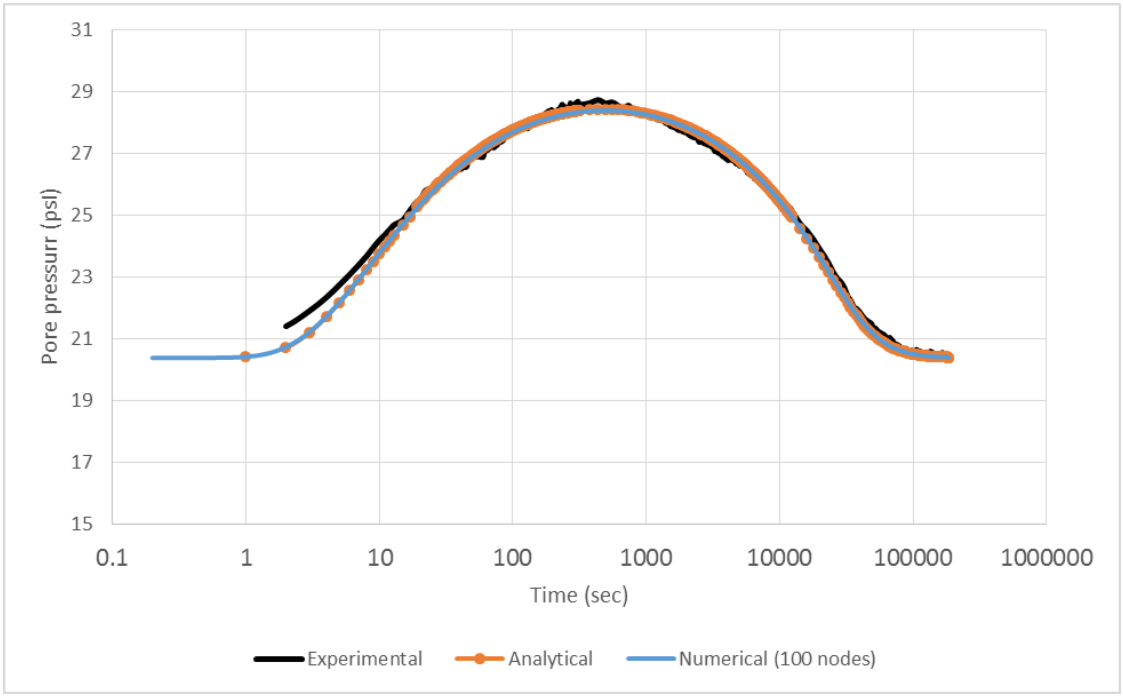

Figure 25 Experimental pore pressure results, analytical and numerical solutions for the specimen under a vertical stress of 30 psi

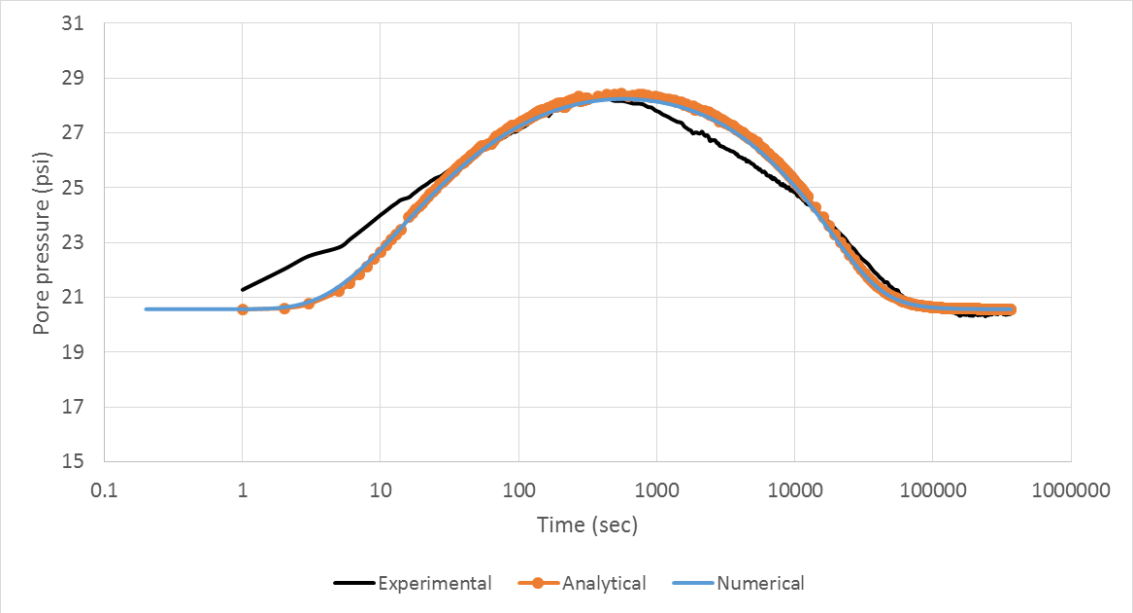

Figure 26 Experimental pore pressure results, analytical and numerical solutions for the specimen under a vertical stress of 40 psi

Figure 27 shows the pore pressure diffusion at the bottom of each one of the 10 elements of the clay specimen under a pressure of 30 psi. It serves as a display to the evolution of the pore pressure propagation across the specimen.

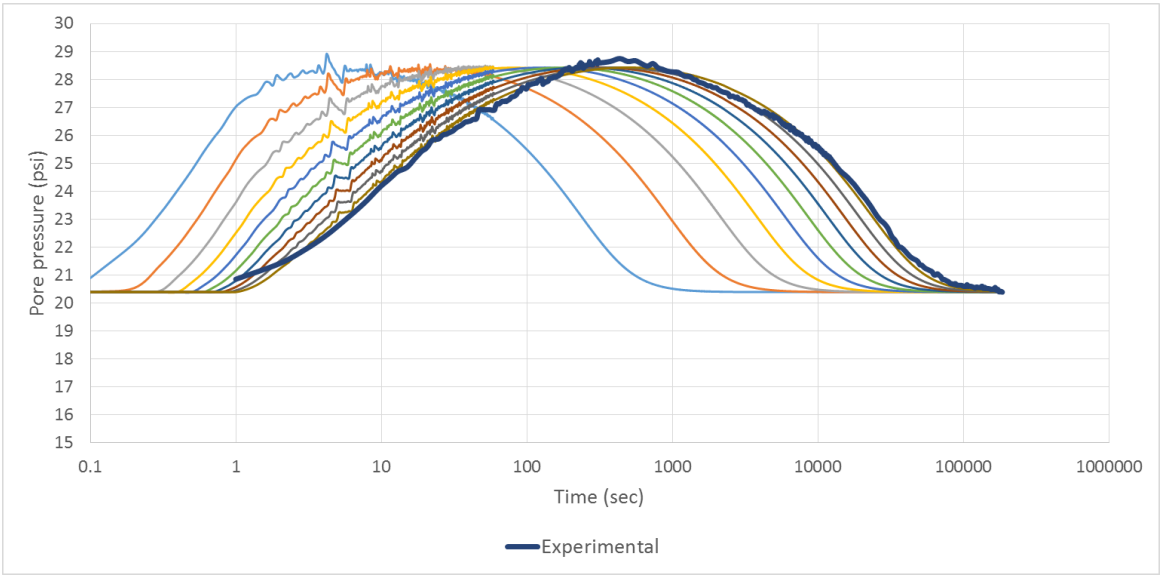

Figure 27 Pore pressure at bottom of each of the 10 elements for the specimen under a 30 psi pressure

As can be seen in Figure 24 to Figure 26, in the first few seconds of each experiment, the different curves do not overlap. The reasoning behind this discrepancy can be related to the nature

of the diffusion equation and what actually happens in the first few seconds experimentally. Specifically, it can be associated with the limitations of applying Biot's theory of poroelasticity under the assumptions that it presents.

Biot described his equations in the context of the Hamiltonian principle of Least Action (Silin & Korneev, 2003). This principle states that the trajectory of a system between an initial and final configuration is found by imagining all the trajectories that can be taken, calculating the action of each trajectory and selecting one that makes the trajectory locally stationary (making the action performed by this trajectory the "least action"). However, using this principle in elastic porous media can be problematic because of the nature of the material in question and Darcy's law that is being implemented. In soils, water flows through a very complex system of geometrically and spatially heterogeneous pore channels. Due to this complex geometry, individual fluid particles accelerate and slow down very abruptly when any sudden changes in the geometry occur. The best speculation that can be thought of in the first few seconds of loading is the fact that the system collapses very instantaneously due to immediate settlement under the load, which disturbs the flow of water.

Another observation that Haneberg (1991) made is that in the case of a shallow impervious substrate (just like the 1" specimen in the lab), high frequency fluctuations propagating downward are amplified at shallow depths, which can lead to an overestimation of the linear-diffusion equations (Haneberg, 1991).

7 CONCLUSION

This thesis discussed the subject of pore water pressure propagation in clays. While pertinent knowledge of the subject of pore pressure diffusion in porous media is abundant in the literature, this research focused on a very specific scenario of pore pressure propagation, where the driving factor is a sudden increase of pore water pressure at the top boundary of a clay layer. This process was compared to the pore pressure propagation encountered during typical consolidation scenarios.

The work discussed in this document is a product of two areas of focus: the analysis of experimental data of pore pressure monitoring of clay specimens under specific drainage and boundary conditions; and the creation of an analytical model, the purpose of which is to describe the theoretical diffusion equation that would best mimic the results obtained in the laboratory. The laboratory tests consisted of a series of pulse tests (where an increase of pore water pressure is applied at the top of a clay) and modified CRS consolidation tests (where the specimens were subjected to increases in total vertical stresses). These two works provided the following findings and conclusions. These conclusions also highlight the research significance and contributions, as well as any future follow-up research:

- A mathematical model was created to describe the pore pressure response in a specimen of clay under an increase of pressure at its top (a pulse setting). This was performed by adopting a Darcian flow with well identified gradient differences. The differential equation describing this process was compared to the equation obtained by Terzaghi in a typical consolidation setting. The difference lies in an additional negative term in the pulse equation, resulting in a time shift in the pore response in a pulse test.
- Pore pressure pulses and consolidation are controlled by diffusion coefficients that are different due to the difference of stiffness ($d\varepsilon/d\sigma'$) in each case. The coefficients c_v(pulse) for pulse tests are higher than c_v(cons) for consolidation tests by orders of magnitude ranging from 0.5 to 1. Meanwhile, the stiffness experienced in a pulse test is higher than that in a consolidation setting by around the same magnitude factors. Future research can further verify this theory, by conducting further pulse and consolidation tests, with both pore pressure and settlement measurements.

- In a CRS consolidation setting, the processes of pore pressure diffusion and consolidation happen simultaneously. As a result of this, any increase of stress $\Delta\sigma$ applied to a clay specimen will not be completely detected at any depth of the clay. As soon as pressure diffuses to a certain depth in the soil, this pressure begins to decrease due to the expulsion of the water. This observation is different from a typical consolidation (or pulse) model where any increase in pressure occurs simultaneously and uniformly at any depth. This highlights the significance of considering time lag effects in consolidation analyses. One very important parameter to consider in this case is the compressibility of the soil under a certain loading. Compressibility has been defined in this text in relation to Biot's theory of poroelasticity, the analysis of which requires looking at the compressibility β of both the solid and the pore matrix. The analysis presented in this document falls short of going deeply into separating the interaction of the solid and the pore phases, and therefore β was best found by optimization so that mathematical models best match the experimental data.

It is important to note that all the models that have been created and applied to experimental data are inherently limited by the nature of Biot's theory of poroelasticity and Darcy's theory of flow. Porous media are intricate systems of heterogeneous pores, varying in both size and distribution, and so the study of flow is very much affected by how complicated this system is. A more meaningful analysis to conduct would consist of a micromechanical approach that considers both the solid and the water phases, an approach that is difficult, time-consuming and impractical for engineering applications anyway.

A future research follow up can consist of further understanding pore pressure diffusion processes in unsaturated media. The presence of air pockets can significantly change the response to pressure changes due to variations in hydraulic conductivity and compressibility. With that in mind, the results of this research are very significant in situations where the medium can be considered very close to saturation, such as in situations of high rainfall over a short period of time. In fact, it is very easy to convert rainfall intensity into pore pressure pulses at the top of a soil surface. The knowledge of pore pressure response in these particular applications is very important in order to predict the pressure needed to cause a landslide failure.

8 APPENDIX

The following is a derivation of the analytical solution to the differential equation (Equation 36) presented in Section 3.2. This equation models the pore pressure in a clay sample as a function of depth and time, as a response to a pulse of pore water pressure at the top of that sample.

The equation to solve is:

$$\frac{\partial \bar{u}}{\partial t} = \frac{k}{m_v \gamma_w} \frac{\partial^2 \bar{u}}{\partial z^2} - \frac{k}{m_v \gamma_w} \frac{1}{dz} \frac{\partial \bar{u}}{\partial z}$$

Where k, m_v and γ_w are constants

dz is the length of the soil profile, taken as L.

To simplify, the equation can be rewritten as:

$$\frac{\partial \bar{u}}{\partial t} = a \frac{\partial^2 \bar{u}}{\partial z^2} + b \frac{\partial \bar{u}}{\partial z}$$

with

$$a = \frac{k}{m_v \gamma_w}$$

$$b = -\frac{k}{m_v \gamma_w} \frac{1}{dz}$$

The boundary conditions are: $\bar{u}$ (0,t) = $\overline{u_i}$ and $\bar{u}$ (L,t) = $\overline{u_i}$

The initial condition is: $\bar{u}$ (z,0) = 0,

The equation can be easier to solve if the boundary conditions are taken to be 0. To satisfy this requirement, the dependent variable $\bar{u}$ can be replaced with v such as:

$$v = \bar{u} - \overline{u_i}$$

$$\frac{\partial v}{\partial t} = \frac{\partial \bar{u}}{\partial t}$$

$$\frac{\partial v}{\partial z} = \frac{\partial \bar{u}}{\partial z}$$

The equation becomes:

$$\frac{\partial v}{\partial t} = a\frac{\partial^2 v}{\partial z^2} + b\frac{\partial v}{\partial z}$$

The new boundary conditions are: v (0,t) = v (L,t) = 0. The initial condition is v (z,0) = $-\overline{u_i}$.

The equation is solved by separation of variables, by taking v (z,t) = Z(z) × T(t).

$$ZT' = aZ''T + bZ'T$$

$$\frac{T'}{T} = a\frac{Z''}{Z} + b\frac{Z'}{Z} = c$$

$$aZ'' + bZ' - cZ = 0 \qquad (1)$$

$$T' - cT = 0 \qquad (2)$$

Solving Equation (1)

The characteristics equation for Equation (1) is $ar^2 + br - c = 0$.

The roots of this equation are:

$$m_1 = \frac{-b + \sqrt{b^2 + 4ac}}{2a}$$

$$m_1 = \frac{-b - \sqrt{b^2 + 4ac}}{2a}$$

The complex conjugate roots are:

$$m_1 = -\frac{b}{2a} + \frac{\sqrt{-b^2 - 4ac}}{2a}i$$

$$m_1 = -\frac{b}{2a} - \frac{\sqrt{-b^2 - 4ac}}{2a}i$$

The general solution is:

$$Z(z) = e^{-\frac{b}{2a}z}\left[c_1 \cos\left(\frac{\sqrt{-b^2 - 4ac}}{2a}z\right) + c_2 \sin\left(\frac{\sqrt{-b^2 - 4ac}}{2a}z\right)\right]$$

(c_1 and c_2 are constants)

Solving Equation (2)

The general solution to Equation (2) is:

$$T = c_3 e^{ct}$$

(c_3 is a constant)

Combining both solutions, the general solution to the partial differential equation is:

$$v(z,t) = e^{-\frac{b}{2a}z}\left[c_4 \cos\left(\frac{\sqrt{-b^2-4ac}}{2a}z\right) + c_5 \sin\left(\frac{\sqrt{-b^2-4ac}}{2a}z\right)\right] \times e^{ct}$$

(c_4 and c_5 are constants)

Constants c, c_4 and c_5 are determined by applying the boundary conditions on the general solution.

$$v(0,t) = e^{-\frac{b}{2a}z}(c_4) = 0$$

$$c_4 = 0$$

$$v(L,t) = e^{-\frac{b}{2a}L}(c_5)\sin\left(\frac{\sqrt{-b^2-4ac}}{2a}L\right)e^{ct} = 0$$

This boundary condition is satisfied when the sin factor is equal to 0. The argument can have values nπ. c_5 is therefore:

$$c = -\frac{an^2\pi^2}{L^2} - \frac{b^2}{4a}$$

Plugging c and c_4 into the solution v(z,t),

$$v(z,t) = c_5 e^{-\frac{b}{2a}z}\sin\left(\frac{n\pi z}{L}\right)e^{\left(-\frac{an^2\pi^2}{L^2}-\frac{b^2}{4a}\right)t}$$

If the solution above yields v (L,t) = 0 for each and every value f n, then we can sum terms for all values of n and still satisfy the boundary conditions.

$$v(z,t) = \sum_{n=0}^{\infty} c_n e^{-\frac{b}{2a}z}\sin\left(\frac{n\pi z}{L}\right)e^{\left(-\frac{an^2\pi^2}{L^2}-\frac{b^2}{4a}\right)t}$$

Constant c_n is determined by accounting for the initial condition: v (z,0) = $-\bar{u}_i$.

$$\sum_{n=0}^{\infty} c_n e^{-\frac{b}{2a}z} \sin\left(\frac{n\pi z}{L}\right) = -\bar{u}_i$$

$$\sum_{n=0}^{\infty} c_n \sin\left(\frac{n\pi z}{L}\right) = -\bar{u}_i e^{\frac{b}{2a}z}$$

The equation above is recognized as a Fourier sine series. The Fourier coefficients are given by:

$$c_n = \frac{2}{L}\int_0^L \bar{u}_i e^{\frac{b}{2a}z} \sin\left(\frac{n\pi z}{L}\right) dz$$

$$c_n = \frac{4a\bar{u}_i\left[2\pi an + be^{\frac{bL}{2a}}\sin(\pi Ln) - 2\pi ane^{\frac{bL}{2a}}\cos(\pi Ln)\right]}{(b^2 + 4\pi^2a^2n^2)L}$$

The final solution to the equation is therefore:

$$v(z,t) = \sum_{n=0}^{\infty} c_n e^{-\frac{b}{2a}z} \sin\left(\frac{n\pi z}{L}\right) e^{\left(-\frac{an^2\pi^2}{L^2} - \frac{b^2}{4a}\right)t}$$

$$\bar{u} = v(z,t) + \bar{u}_i$$

With a, b and c_n are defined previously.

9 REFERENCES

Ba, J., Carcione, J. M., & Nie, J. X. (2011). Biot-Rayleigh theory of wave propagation. *Journal of geophysical research.*

Berti, M., & Simoni, A. (2009). Field evidence of pore pressure diffusion in clayey soils prone to landsliding. *Journal of geophysical research*.

Brewster, A. (2015). *Using Coefficient of Consolidation to Assess Response Time and Reading Accuracy of Piezometers in Grouted Boreholes in Fat Clays.*

Corapcioglu, Y., & Tuncay, K. (1996). Propagation of waves in porous media. *Transport in Porous Media*.

Detournay, E., & H.-D. Cheng, A. (1993). Fundamentals of Poroelasticity. *Comprehensive Rock Engineering: Principles, Practice and Projects*.

Dullien, F. A. (1991). *Porous Media: Fluid transport and pore structure.*

Eaton, D. W. (2011). *2-D Finite-difference Modelling of Pore-pressure Diffusion in Heterogeneous.*

Feng, T.-W. (2010). Some Observations On The Oedometric Consolidation. *Journal of GeoEngineering*.

Haneberg, W. C. (1991). *Pore Pressure Diffusion and the Hydrologic Response of Nearly Saturated, Thin LandslideDeposits to Rainfall.* The Journal of Geology.

Iverson, R. M. (2000). Landslide triggering by rain infiltration. *Water resources research.*

Iverson, R. M. (2005). Regulation of landslide motion by dilatancy and pore. *Journal of geophysical research*.

Katsube, T. (2010). Review of formation resistivity factor equations related to new pore-structure concepts. *Geological Survey of Canada*.

Lancellotta, R. (2002). Coupling between the evolution of a deformable porous medium and the motion of fluids in the connected porosity. In W. Ehlers, & J. Bluhm, *Porous media : theory, experiments, and numerical applications* (pp. 199-225).

Reid, M. (1994). A Pore-Pressure Diffusion Model for Estimating Landslide-Inducing Rainfall. *The Journal of Geology*.

Reservoir Engineering Online. (2014). Retrieved from Reservoir Online: http://reservoironline.blogspot.com/2014/08/porosity.html

Silin, D., & Korneev, V. (2003). *Pressure diffusion waves in porous media.* Lawrence Berkeley National Laboratory.

Tang, L., Chen, H., & Song, J. (2016). Process of pore pressure diffusion in saturated clay soil and impact of adsorbed. *Geosciences Journal*.

Van der Grinte, J., Van Dongen, M., & Van der Kogel, H. (1987). Strain and pore pressure propagation in a water-saturated porous medium. *Journal of Applied Physics*.

Yang, D., Li, Q., & Zhang, L. (2015). Propagation of pore pressure diffusion waves in saturated porous media. *Journal of Applied Physics*.